# UNIVERSITY OF PADOVA

**DEPARTMENT OF**

**INFORMATION ENGINEERING**


FINAL MASTER'S DEGREE REPORT

# DEVELOPMENT OF MUSCULOSKELETAL MODEL FOR BIOMECHANICAL ANALYSIS OF TRANS-TIBIAL AMPUTEE GAIT


Supervisor: Ing. NICOLA PETRONE

Co-Supervisor: Prof. UWE KERSTING

Student: ENRICO NUCIBELLA



ACADEMIC YEAR 2009-10

# Table of Contents


Chapter 1…… 7

Introduction……..... 7

1.1 Previous studies……... 8

1.1.1 Kinematics…… 9

1.1.2 Moment of force…….. 11

1.1.3 Power outputs…….. 14

1.1.4 Electromyographic activity…….. 17

1.2 Purpose of this project……. 21

Chapter 2…… 23

Prosthetic feet used during the data collection…….. 23

2.1 Introduction……. 23

2.2 S.A.C.H. foot…….. 24

2.2.1 Structural characteristics……... 24

2.2.2 Advantages and disadvantages…… 26

2.3 Greissinger foot……... 27

Chapter 3…… 31

Materials and methods……... 31

3.1 Gait Lab……... 31

3.2 Subjects……... 32

3.3 Procedures……... 33

3.3.1 Preparation of the subjects……..... 33

3.3.2 Data collection…….…. 34

3.4 Data analysis…….…... 36

3.4.1 Procedure to achieve the results…….…... 36

3.4.2 Selection of the events…….…… 37

3.4.3 Development of *virtual amputee* …… ……..…… 38

Chapter 4…….. ..... 39

Inverse Dynamics…….... 39

4.1 Forward and Inverse Dynamic……..……39

4.2 Muscle recruitment……... 39

4.3 AnyBody Modeling System…….. 41
4.3.1 AnyScript modeling language…… 42
Chapter 5…….. 45
Development of the model……... 45
5.1 Repository…….. 45
5.1.1 GaitLowerExtremity characteristics……... 45
5.2 Generation of an individualized leg-stump model…… 48
5.2.1 Generation of the “LegTD_Amputee” folder…… 48
5.3 Generation of the “Prosthesis” folder……... 53
5.3.1 Prosthetic shank……. 53
5.3.2 Prosthetic foot…… 54
5.3.3 Generation of the joints…….. 55
Chapter 6……. 57
Results……. 57
6.1 Stride characteristics……. 57
6.2 Comparison normal subject and amputees……... 58
6.2.1 Ground reaction forces…….. 58
6.2.2 Joint angles…… 60
6.2.3 Joint moments…… 63
6.2.4 Power……. 66
6.2.5 Muscular activity…… 70
6.3 Comparison amputee group and virtual amputee ……..……... 74
6.3.1 Joint moments……. 74
6.3.2 Power……. 76
6.3.3 Muscular activity…… 78
6.4 Discussion……. 82
6.4.1 Review of the results…….. 82
6.4.2 Discussion of the results……. 83
6.5 Conclusions……... 86
Appendix A…… 87
List of References…….. 91

# List of Tables

Table 1.1 Subjects characteristics mean (SD) …… 10
Table 1.2 Stride characteristics mean (SD) …… 10
Table 2.1 S.A.C.H. foot characteristics …… 27
Table 2.2 Greissinger foot characteristics …… 29
Table 3.1 Subjects characteristics mean (SD) …… 32
Table 3.2 Anthropometric parameters …… 33
Table 3.3 Marker label, description and position (only left side markers are listed, the positioning of the right side is identical) …….. 34
Table 6.1 Stride characteristics …….. 57

# List of Figures

Figure 1.1 Knee motion averages for trans-tibial amputee and control group …….. 11
Figure 1.2 Moment of force for normal subjects. The stride period was normalized to 100%, and stance time to 60%. Solid line shows the average curve, dotted line is one standard deviation either side of the mean …….. 12
Figure 1.1 Averages of moment of force of eight amputee trials …….. 12
Figure 1.4 Moment of force for amputees (S.A.C.H. foot) …… 13
Figure 1.5 Moment of force for amputees (Greissinger foot) …… 13
Figure 1.6 Average of knee moment of force for the trans-tibial amputee and the control group. Positive values indicate a flexion moment, while negative values indicate an extension moment …… 14
Figure 1.7 Mechanical power averages for the control group ……... 16

Figure 1.8 Averages of mechanical power of eight amputee trials ……... 16
Figure 1.9 Power patterns (S.A.C.H. foot) ……... 16
Figure 1.10 Power patterns (Greissinger prosthesis) …… 16
Figure 1.11 Average of knee power for the trans-tibial amputee and the control group ……..... 17
Figure 1.12 Averages of EMG signal. S.A.C.H. foot (dashed line), normal group (solid line for average, dotted line for one standard deviation) ……..... 18
Figure 1.13 Mean EMG profiles of vastus lateralis for trans-tibial amputee and control group (% MMT = percentage of maximal muscle test) …… 20
Figure 1.14 Mean EMG profiles of semimembranosis for trans-tibial amputee and control group (% MMT = percentage of maximal muscle test) ……..... 20
Figure 1.15 Mean EMG profiles of biceps femoris long head for trans-tibial amputee and control group (% MMT = percentage of maximal muscle test) …….. 20
Figure 2.1 S.A.C.H. foot ……... 24
Figure 2.2 Sagittal section of the S.A.C.H. foot. A=the carriage bolt, three-eighths of an inch in diameter, with the head embedded in the keel; B=wooden keel; C=laminated cushioned rubber heel; D=belting between neoprene outer cover

and wooden keel; E=neoprene toe …… 26
Figure 2.3 Greissinger foot multiple-axis assembly …… 28
Figure 3.1 VICON cameras …….. 31
Figure 3.2 AMTI force platform ……... 32
Figure 3.3 Plug-in marker placement protocol ……..... 35
Figure 4.1 Example of a full body model ……..... 42
Figure 4.2 Tree structure that shows the grouping of the models ……..... 43
Figure 4.3 Example of a structured model. The two bicycle are identical applications, and are combined with a 2D lower extremity (left), and a 3D lower extremity (right) ……..... 44
Figure 5.1 First part of the code of GaitLowerExtremity.any file. The operator can chose to run the MotionAndParameterOptimizationModel, or the InverseDynamicModel …….. 46
Figure 5.2 Example of a lower extremity model. The blue markers are those from the c3d file, while the red ones are the markers of the model ……... 47
Figure 5.3 Example of a tibia. The red part is selected, and it's going to be removed ……..... 49
Figure 5.4 Example of tibia. The distal part of the tibia is been removed ……..... 50
Figure 5.5 Skeleton model with the lower part of the tibia that is cut …….. 50
Figure 5.6 Reference to the LegTD_Amputee folder ……..... 52
Figure 5.7 Prosthetic shank ……... 54
Figure 5.8 Amputee model view …… 56
Figure 6.1 Vertical component of the ground reaction force during stance phase…….. 59
Figure 6.2 Anterior-posterior component of the ground reaction force during stance phase .. 59
Figure 6.3 Medial-lateral component of the ground reaction force during stance phase ..... 60
Figure 6.4 Knee flexion-extension during stance phase..... 61
Figure 6.5 Hip flexion-extension during stance phase..... 62
Figure 6.6 Hip abduction-adduction during stance phase ..... 63
Figure 6.7 Knee moment in the sagittal plane, during stance phase ..... 64
Figure 6.8 Hip moment in the sagittal plane, during stance phase ..... 65
Figure 6.9 Hip moment in the frontal plane, during stance phase..... 66

Figure 6.10 Knee power in the sagittal plane ..... 67
Figure 6.11 Hip power in the sagittal plane ..... 68
Figure 6.12 Hip power in the frontal plane ..... 69
Figure 6.13 Vastus lateralis activation during stance phase ..... 70
Figure 6.14 Vastus medialis activation during stance phase ..... 71
Figure 6.15 Biceps femoris activation during stance phase ..... 73
Figure 6.16 Right gluteus maximus (superior) activation during stance phase ..... 73
Figure 6.17 Knee moment in the sagittal plane, during stance phase ..... 74
Figure 6.18 Hip moment in the sagittal plane, during stance phase ..... 75
Figure 6.19 Hip moment in the frontal plane, during stance phase ..... 76
Figure 6.20 Knee power in the sagittal plane ..... 76
Figure 6.21 Hip power in the sagittal plane ..... 77
Figure 6.22 Hip power in the frontal plane ..... 78
Figure 6.23 Vastus lateralis activation during stance phase ..... 79
Figure 6.24 Vastus medialis activation during stance phase ..... 80
Figure 6.25 Biceps femoris activation during stance phase ..... 81
Figure 6.26 Right gluteus maximus (superior) activation during stance phase ..... 82

# Chapter 1.

# Introduction

The number of below knee amputees in our population is not negligible. In the United States, for instance, there are currently approximately 350,000 amputees (ref).

The major reasons that cause an amputation of the lower limbs are: disease, trauma, congenital or birth defects, and tumors.

Specifically, the conditions that lead to amputation of an extremity of the body can be:

- impaired circulation as a complication of diabetes mellitus;
- hardening of the arteries;
- arterial embolism;
- gangrene;
- severe frostbite;

There are two major contextual circumstances leading to amputations, those that are planned, and the amputations that are the result of emergency procedures after an accident. In the second case the main causes are injuries and arterial embolisms.

In general, amputation as surgical operation is conducted in two steps. First, an incision is made at the level where the amputation is planned. The bone in that point is cut and smoothed. A flap made of muscle, connective tissue and skin covers the bone, and will be closed with some sutures.

The second step is to create a stump to make possible the attachment of the prosthesis, or an other prosthetic device.

The task of the surgeon is to find the best place where the amputation should be made. This procedure is very important to accommodate tissue healing, and try to retain the maximum amount of limb for the re-education treatment. This is an important step of the amputation procedure. There is a risk for infection associated with the orthopaedic procedure. A possible consequence is

that there might be infections. The surgeon in this case has to remove the prosthesis, and sometimes to amputate a second time at a higher level.

If the operation was successful, the rehabilitation training should start as soon as possible.

It may be very difficult for the patient to start moving after the surgery, however, this is important for the blood circulation, maintaining muscle activity to counteract atrophy.

Initially it may be very difficult to follow the training program, especially because of the high chances for psychological problems in the patient. However, this will not be discussed in this report.

The differences in ambulation between a normal person and an amputee are considerable. That is why the collaboration between physiotherapist and engineer is of great importance.

The patients show asymmetries that can be different. It depends of the cause of the amputation. If, for instance, the cause of the amputation is an accident, the patient loses suddenly the limb. In this case the physiotherapist should train the patient adopting particular exercises, such that the amputee can familiarize him- or herself with the prosthesis and correct for the asymmetries that he or she demonstrates.

If the cause of the amputation is illness, diabetes for example, the process leading to the amputation usually develops over a long time period. In this case the physiotherapist has to re-educate the patient to walk in a correct way.

The purpose that the physiotherapic group has is to correct the gait of amputees, and make it more symmetric than possible.

Sometime this way to proceed is not so careful. A correct movement is not always synonymous of “right work” of the joints.

As Czerniecki et al. (1996) described, the amputee can achieve a symmetric gait, but, doing this, there is a possible overloading in the contralateral joints.

This compensation can be the cause of future surgery, for instance the replacement of the hip.

## 1.1 Previous studies

There are several reports on the biomechanics of amputee gait available in the literature.

Winter et al. (1988) conducted biomechanical and EMG analyses from below knee amputee (BK). The prostheses used by the subjects had ankle mechanisms with limited or no rotation which provided some ankle stability.

The main consequence of a trans-tibial amputation is that the patient loses the plantarflexors. These muscles, in the early stance, control the forward rotation of the leg over the supporting foot. They are also responsible for over 80% of mechanical power generated during the gait cycle.

The purpose of this study was to observe if there were any compensations and asymmetries in the movements of hip and knee during gait cycle.

All five subjects used the S.A.C.H. (Solid Ankle Cushion Heel) prosthetic foot. This is a non-articulated assembly where the foot and the ankle are combined together with a compressible heel.

One of the subjects tried also a Greissinger fitting. Therefore, this study gives limited possibilities for a systematic comparison between prosthesis types but provides some insights into the effects on different prostheses.

An other important study was published by Powers et al. (1998), where the mechanics of the knee during gait were evaluated. Also in this case, the subjects that Powers et al. considered were patients that showed a trans-tibial amputation (TTA). The results were compared with the data from a group of sound people.

### 1.1.1 Kinematics

Powers et al. observed that the TTA group walked with a slower velocity (63.5 vs. 77.8 m/min) than the control group, and showed a reduced stride length (1.21 vs. 1.42 m). The TTA group showed a longer heel only contact (20.6% of the gait cycle) than control group (12.1% of the gait cycle). All the subjects presented the same stance and initial double support times.

The main differences between the knee motion patterns of the two groups were in the first 40% of the gait cycle. The peak that represented the flexion of the TTA knee is less compared with the normal group (9.5 vs. 18.6°). It can be seen that this peak occurred with a short delay (17.3 vs. 13.2% of the gait cycle).

*Table 1.1. Subjects characteristics mean (SD)*

Table 1
Subject characteristics mean (S.D.)

| | TTA group ($n = 10$) | Control group ($n = 10$) |
|---|---|---|
| Age (y) | 62.3 (6.9) | 50.9 (8.6) |
| Height (m) | 1.8 (0.08) | 1.7 (0.09) |
| Weight (kg) | 90.7 (15.5) | 72.8 (10.1) |

*Table 1.2. Stride characteristics mean (SD)*

Table 2
Stride characteristics mean (S.D.)

| | TTA group ($n = 10$) | Control group ($n = 10$) | $p$-value |
|---|---|---|---|
| Velocity (m/min) | 63.5 (11.0) | 77.8 (11.9) | 0.01 |
| Cadence (steps/min) | 104.9 (8.9) | 109.3 (13.5) | 0.40 |
| Stride length (m) | 1.21 (0.17) | 1.42 (0.11) | 0.003 |
| Stance time (% GC) | 63.3 (2.6) | 64.4 (1.8) | 0.31 |
| IDLS time (% GC) | 15.7 (2.8) | 14.0 (1.8) | 0.12 |
| Heel only time (% GC) | 20.6 (8.4) | 12.1 (5.0) | 0.013 |

TTA, trans-tibial amputee.
% GC, percent gait cycle.
IDLS, initial double limb support.

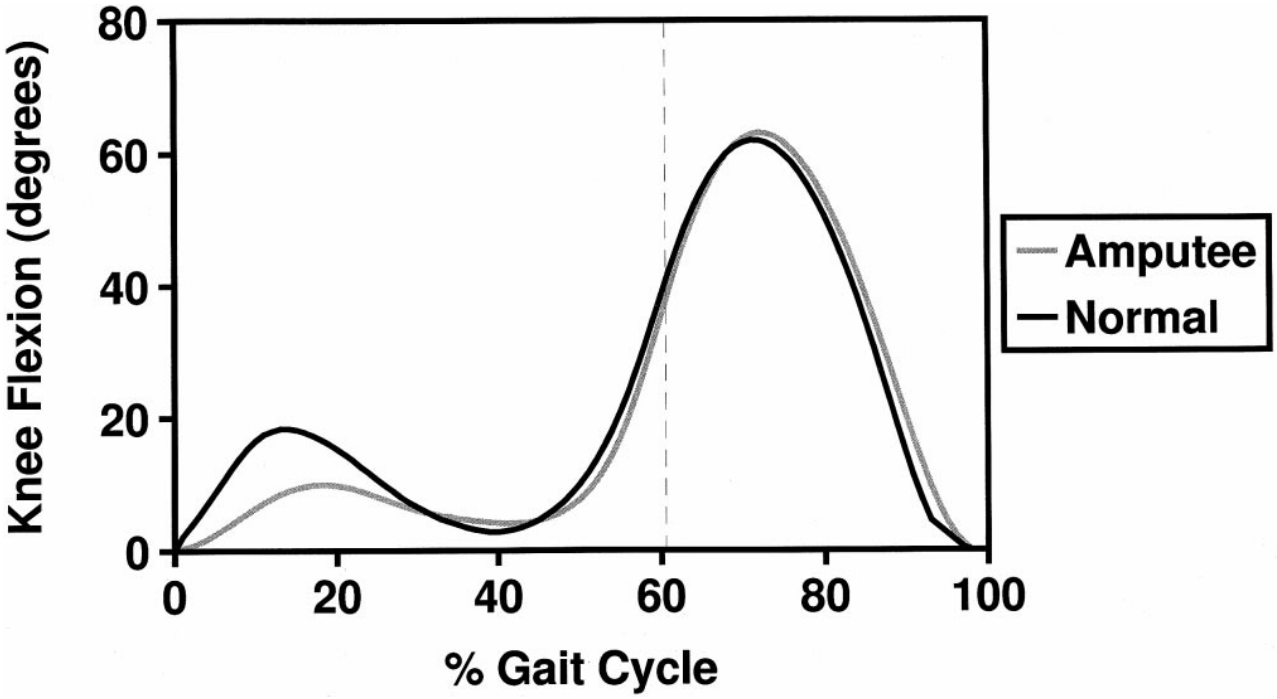


*Figure 1.1. Knee motion averages for trans-tibial amputee and control group*

### 1.1.2 Moment of force

The moment of force profiles for the sound patients that have been achieved in the study of Winter et al. are shown in Figure 1.2.

The convention is that the extensor moments were positive, and the flexor moments were negative. All the amputees presented a dorsiflexor moment at the ankle for first 18% of stride (6% for normal group).

Sound patients were faster in lowering the foot to the ground, and this movement was controlled by the muscles dorsiflexors. The rigid ankles that characterized the prosthetic feet used by the amputees generated an internal dorsiflexor moment from heel contact to the instant when the prosthetic foot was flat on the ground. That proceeding to rotate forward the amputee leg took more time than in the normal subjects.

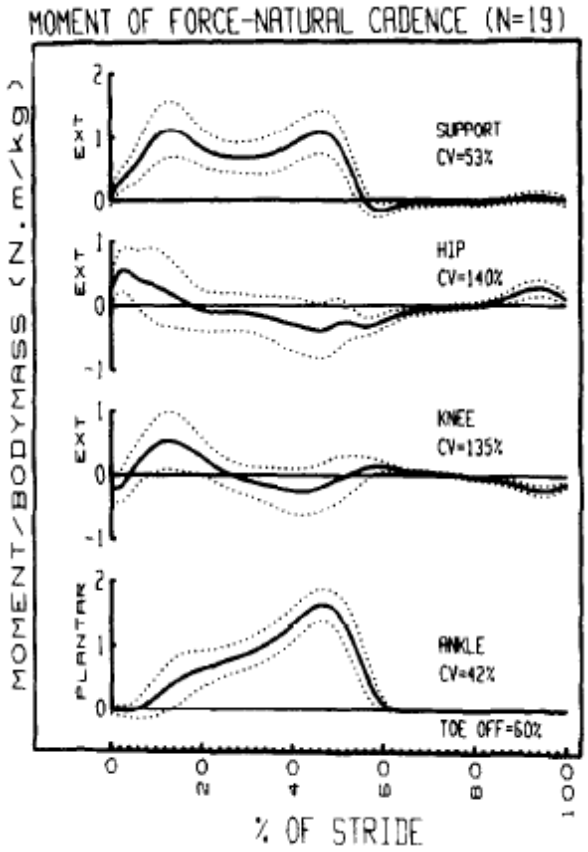


*Figure 1. 2. Moment of force for normal subjects. The stride period was normalized to 100%, and stance time to 60%. Solid line shows the average curve, dotted line is one standard deviation either side of the mean.*

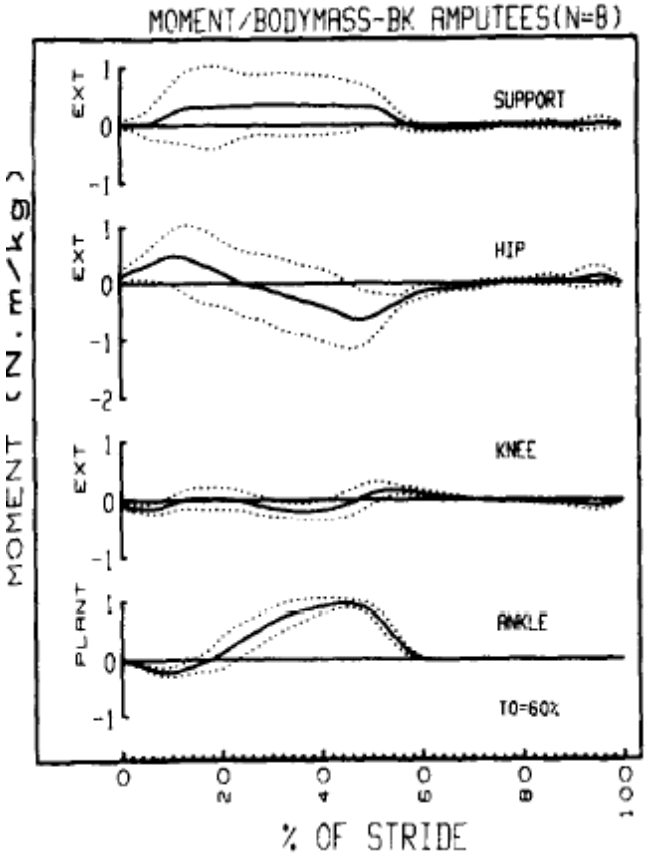


*Figure 1.3. Averages of moment of force of eight amputee trials.*

About the knee, the moment of force was very low during the first half of stance, with an exception for the Greissinger foot (Figure 1.5).

The hip moment of force in the amputees showed more variability than the normal group.

Only the amputee that used the Greissinger foot showed a normal hip moment pattern, while three SACH trials presented an extensor pattern during stance phase, the other two SACH and the Uniaxial trials had above normal flexor moments.

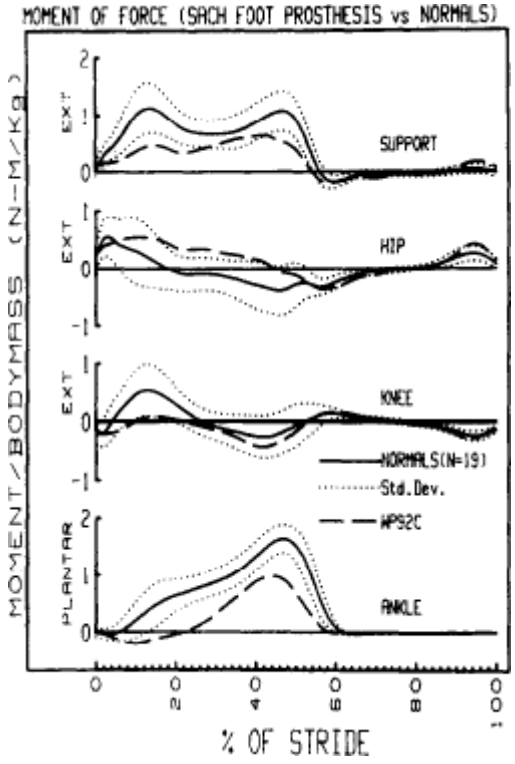


*Figure 1.4. Moment of force for amputees (S.A.C.H. foot).*

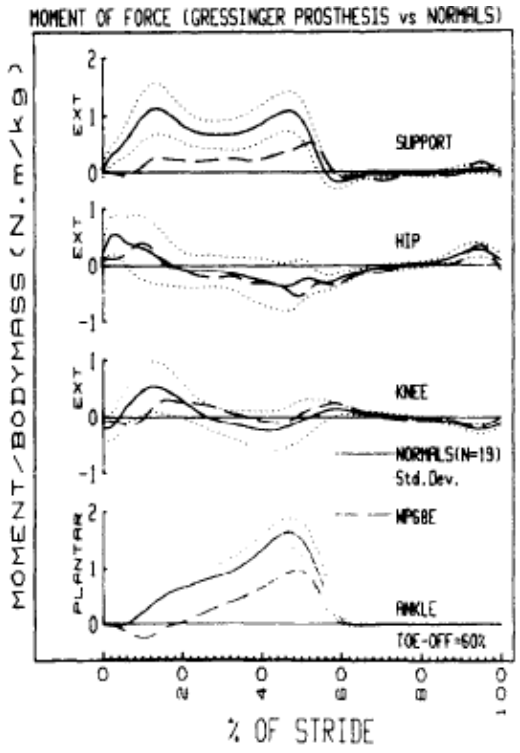


*Figure 1.5. Moment of force for amputees (Greissinger foot).*

In the study of Powers et al. the control group showed a flexion moment of force during the stance phase. Only brief periods of extension moment after the initial contact and at the 40% of the gait cycle. The TTA group presented knee flexion moment only in two points of the stance phase (16% and 57%).

The greatest difference between the moment of force of the two groups of subjects occurred in the early stance phase, where the peak presented by the amputees is significantly less than normals (0.05 vs. 0.70 N-m/kg-m). There were not great differences in the timing of the flexion moment peaks (15.7% for the TTA group, and 14.2% for the control group).

During the swing phase the moment patterns are almost the same. There was only a greater extension moment presented by the normal group (95% of the gait cycle).

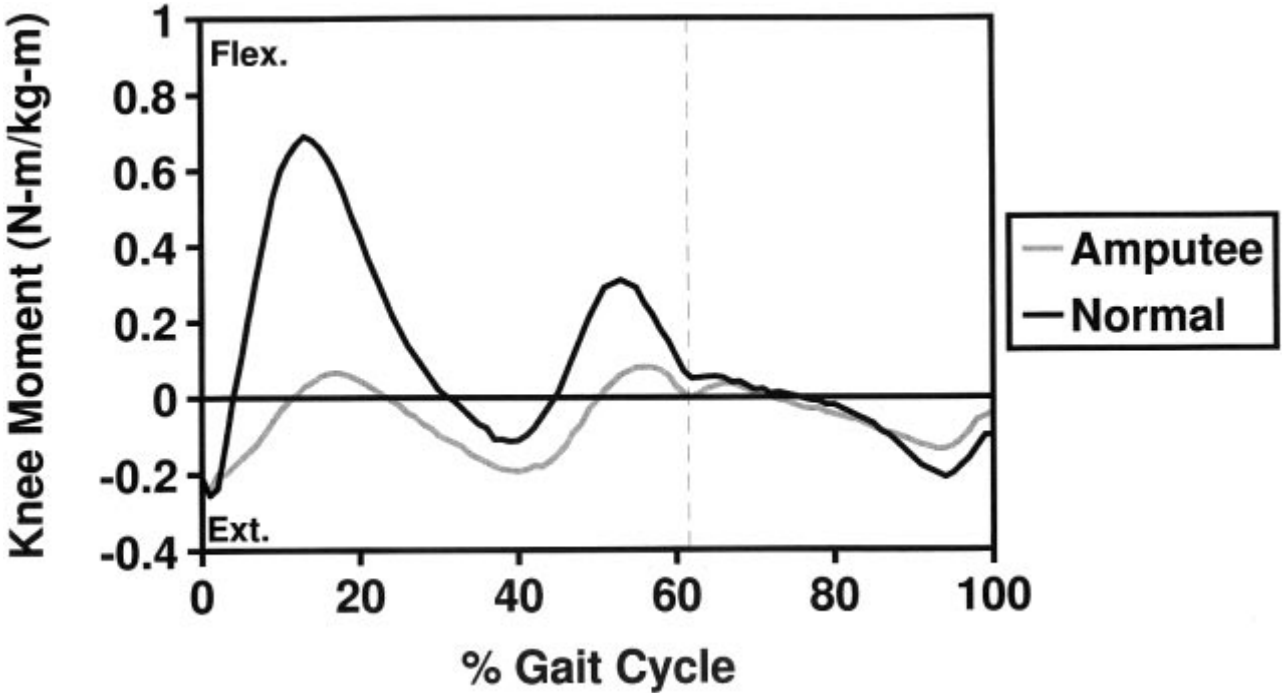


*Figure 1.6. Average of knee moment of force for the trans-tibial amputee and the control group. Positive values indicate a flexion moment, while negative values indicate an extension moment.*

### 1.1.3 Power outputs

In both the studies that I considered the power of the joints was achieved by using this formula:

$P_j = M_j \cdot \omega_j$,

where the power, represented by $P_j$, was positive if the moment of force, $M_j$, and the angular velocity, $\omega_j$, had the same polarity. $P_j$ was negative in the case that $M_j$ and $\omega_j$ had opposite polarity. Positive power represented the generation of energy during a concentric contraction, whereas a negative power showed an absorption of energy during an eccentric contraction.

In the case of amputees, positive power indicated the return of stored energy from the mechanism that characterizes the prosthesis. The negative power reflected the absorption of energy by that mechanism (damper, spring).

The power curves were reported in $Wkg^{-1}$, and were normalized to body mass.

Winter et al. observed that the prosthesis absorbed energy when the foot deformed slightly in dorsiflexion during mid stance. This absorption of energy is established by the plantarflexors as soon as the leg rotates forward over the foot flat. This is presented with the curve A1 in Figure 1.8. This energy absorbed was dissipated in the viscous material of the SACH foot, or stored in the mechanisms of the Uniaxial and Greissinger feet. Some of the spring mechanisms returned energy generated during push off. Curve A2 presents the generation of energy by muscles plantarflexors (when the foot plantarflexed prior to the toe-off).

In all the amputees, the absorption of energy by knee extensors when the knee flexed during the weight acceptance (K1), and energy generation by knee extensors when the knee extended during mid stance to raise the center of gravity of the body (K2) were missing.

The absorption done by knee extensors during push-off (K3) is almost similar to the normal group, while the energy absorption by the knee flexors at end of swing was negligible in all amputees but one. Also the power output characteristics related to the hip showed a high variability, especially when a brief hip generation by hip extensors at weight acceptance (H1), and an absorption done by hip flexors (H2) occur.

After heel contact the mean pattern showed an H1 burst as the hip extensors shortened, and generated energy useful to induce the body forward. This energy generation is an important compensation for the absence of energy generation by the muscles plantarflexors of the ankle.

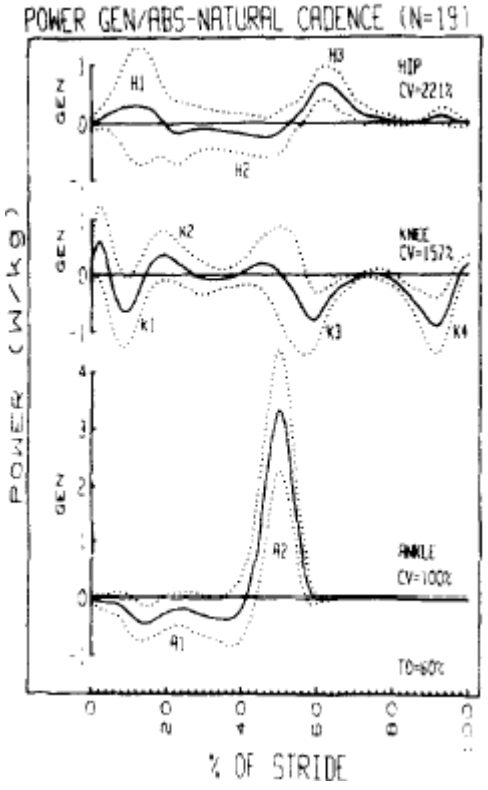


*Figure 1.7. Mechanical power averages for the control group.*

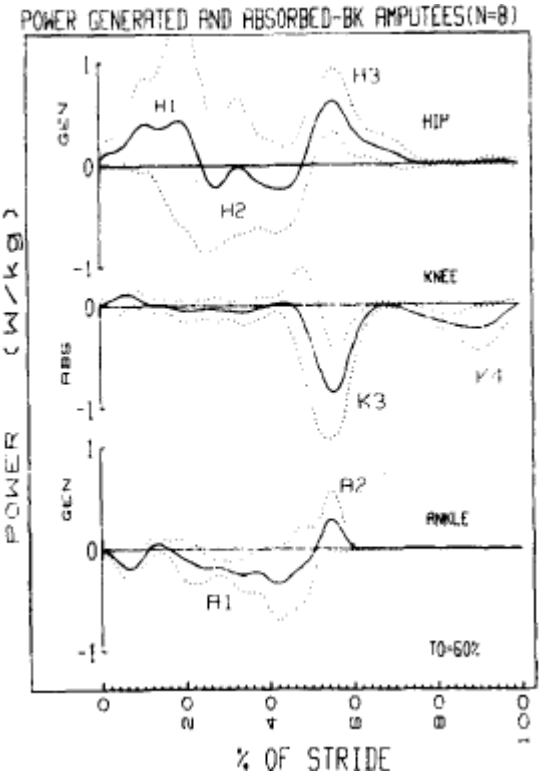


*Figure 1.8. Averages of mechanical power of eight amputee trials.*

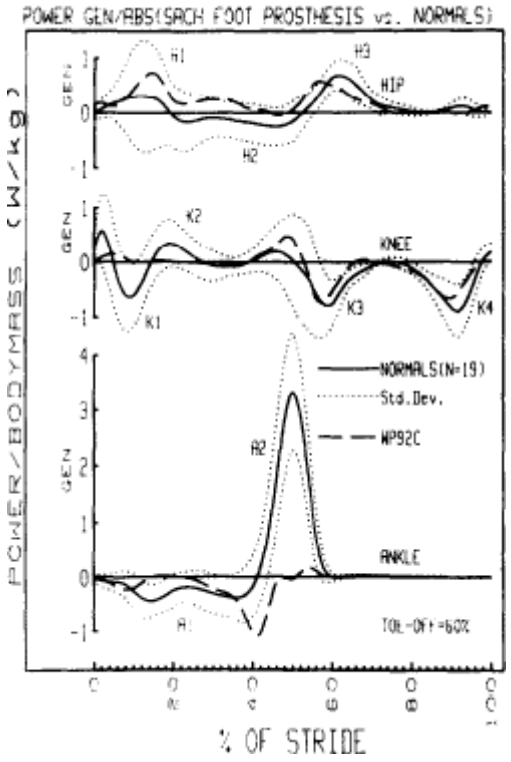


*Figure 1.9. Power patterns (S.A.C.H. foot).*

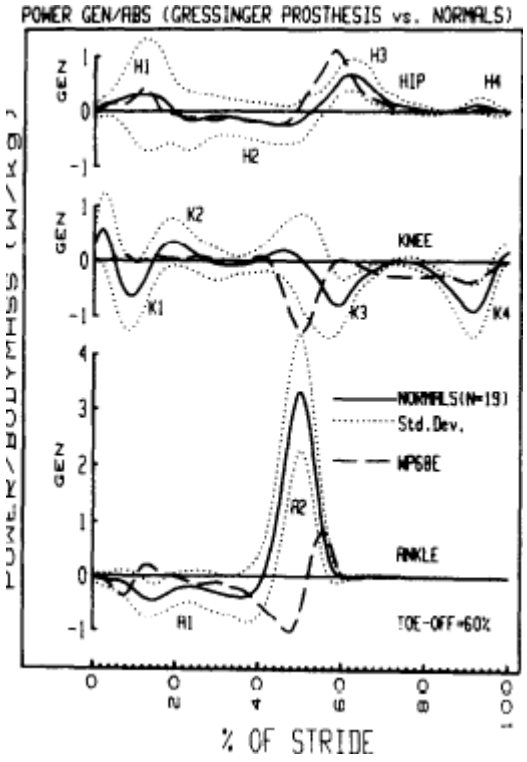


*Figure 1.10. Power patterns (Greissinger prosthesis).*

At the knee, Powers et al. observed that the TTA group showed a near zero power curve, while the control group presented a great positive power burst at 11% of the gait cycle and three negative power peaks (5, 20 and 51% of the gait cycle).

The biggest difference about the knee power patterns was in the initial contact, where the control group presented a peak that was greater (0.6 W/kg-m) than the TTA group (0.08 W/kg-m).

The timing of the peak positive power occurred earlier in the TTA group than in the control group (2.5 vs. 11% of the gait cycle).

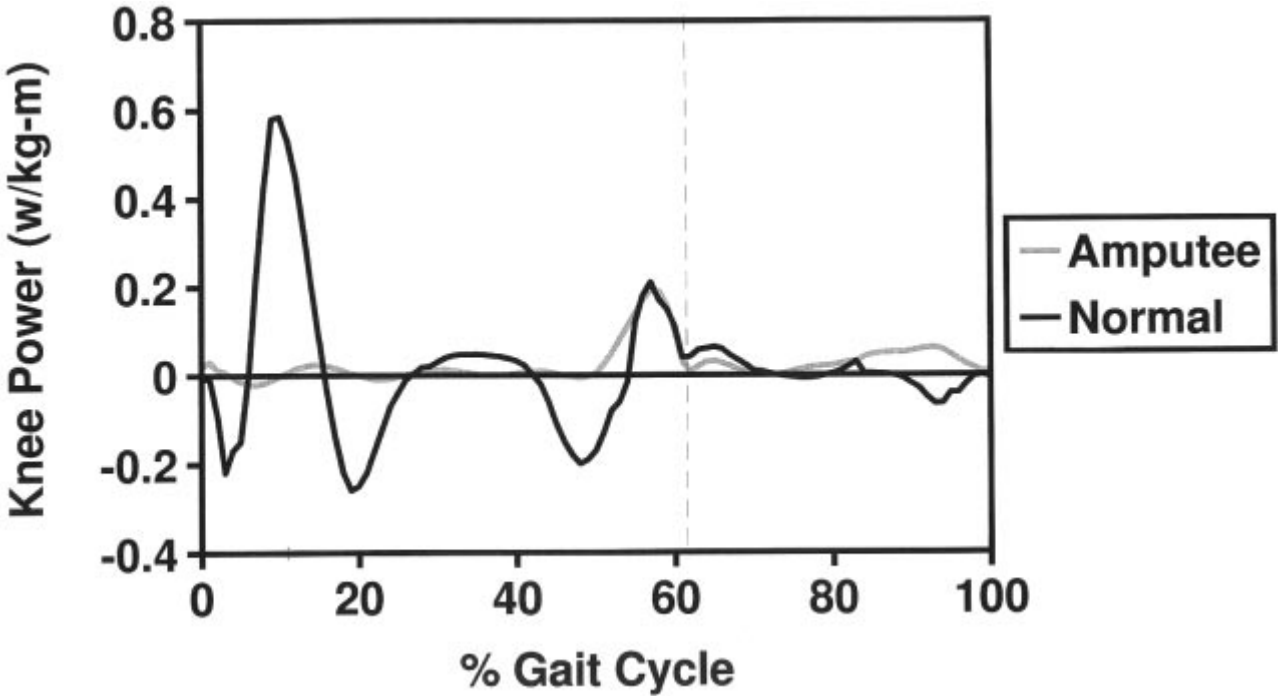


*Figure 1.11. Average of knee power for the trans-tibial amputee and the control group.*

### 1.1.4 Electromyographic activity

Winter et al. observing the electromyographic (EMG) analyses discovered that in the amputee group the extensors of the hip were dominant for most of stance. This is showed by the hip moment of force pattern and the hyperactivity of the muscles gluteus maximus, biceps femoris and semitendinosis.

This group of muscles generated an above normal knee flexor moment (in the first 40% of the stride period).

The EMG also showed a hyperactivity of the knee extensors (vastus lateralis, rectus femoris). This indicated a major contraction at the knee joint. The co-contraction against the flexors of the knee caused the net knee moment during stance to be near zero, and this could be interpreted as a stiffening of the knee joint.

During push-off (40-60% of stride period) the flexors of the knee were less active, while the extensors were well activated into swing. This resulted in a net knee extensor moment which controlled the knee as it flexed at that time.

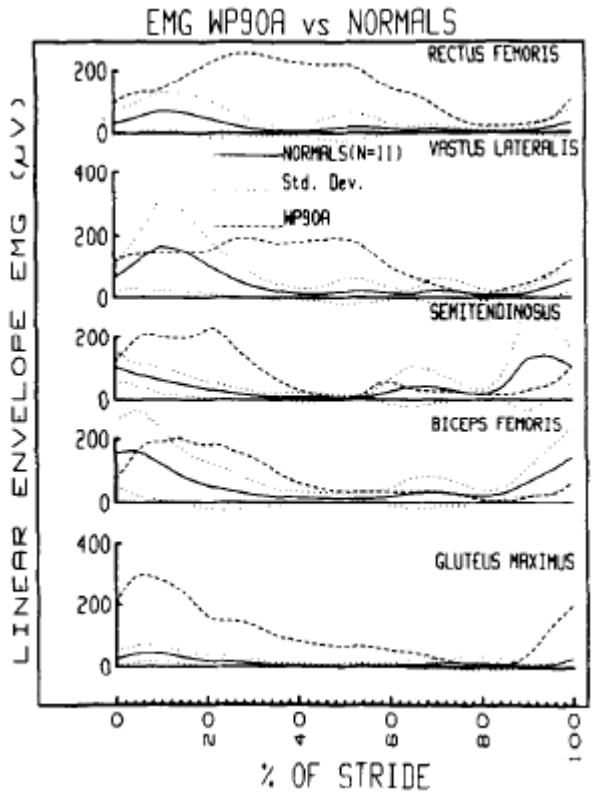


*Figure 1.12. Averages of EMG signal. S.A.C.H. foot (dashed line), normal group (solid line for average, dotted line for one standard deviation).*

In the study of Powers et al., the amputee group presented a greater muscular activity than the normal group. This was in contrast with the reduced moment of force and mechanical power at the knee.

These results are in agreement to those reported in the study of Winter et al., that demonstrated that the reduced moment of force is a consequence of a co-contraction of the biceps femoris and the quadriceps.

The TTA group showed a greater EMG activity for all the muscles that were tested (vastus lateralis, biceps femoris long head, semimembranosis).

The mean EMG intensity for all the muscles of the TTA group was 40% MMT (percentage of maximal muscle test) against the 29% MMT for the control group.

The semimembranosis of the amputees presented an EMG intensity of 45% MMT, while the sound people showed an intensity of 31% MMT.

We can observe from the graphs that there were some differences between the duration of the muscles activation during the gait cycle.

The greatest difference in the duration of activity was in the long head of the biceps femoris. This muscle in the TTA group worked until the 56% of the gait cycle in the amputee patients, while in the sound people it worked until the 13% of the gait cycle.

The EMG data of control group confirmed that there was a demand of extensors muscles to control the flexion of the knee during the weight acceptance. We can observe this from the activity of the vastus lateralis which had an average intensity of 29% MMT (until 22% of the gait cycle).

In the TTA group the moment of force data showed a negligible extensors demand, and a little flexion of the knee during the stance phase. Checking the EMG data of the TTA group, the vastus lateralis presented a greater activity than in the control group. The intensity increased of 25% MMT in the average, and duration of the activity is longer than control group (lasting until 33% of the gait cycle).

One of the possible reasons of the greater EMG activity presented by the TTA group was the decreased mobility of the prosthetic foot, especially during weight acceptance.

During normal gait, there is a plantarflexion of 10° after initial contact which provides foot flat contact with the floor. In this phase the weight of the body can be transferred to the supporting limb. The TTA group spent the first 20% of the gait cycle with heel only contact. The foot flat phase presented a delay in this group

The inability shown by the TTA group to achieve a foot flat posture during loading response could be attributed to the compromised plantarflexion of the Seattle LightFoot (that provided only 2-3° of motion).

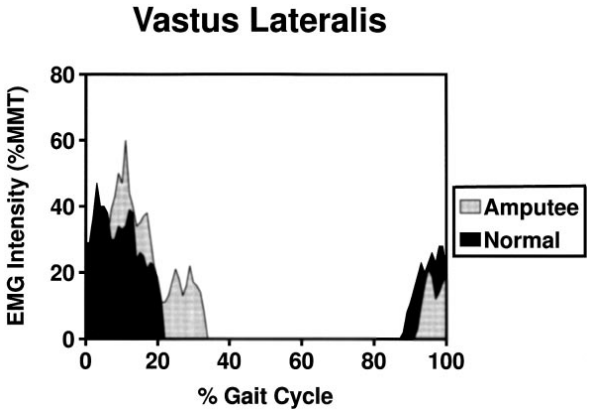


*Figure 1.13. Mean EMG profiles of vastus lateralis for trans-tibial amputee and control group (% MMT = percentage of maximal muscle test).*

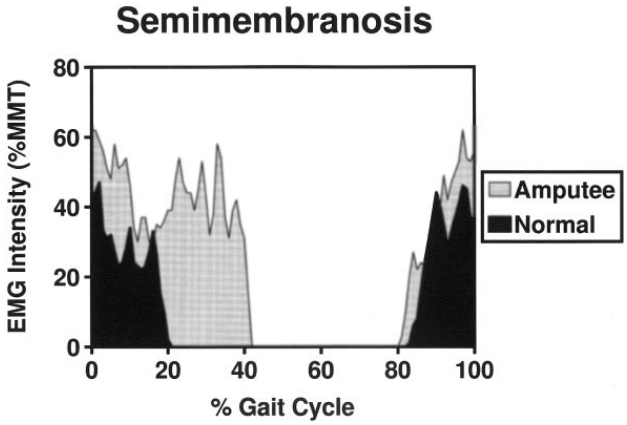


*Figure 1.14. Mean EMG profiles of semimembranosis for trans-tibial amputee and control group (% MMT = percentage of maximal muscle test).*

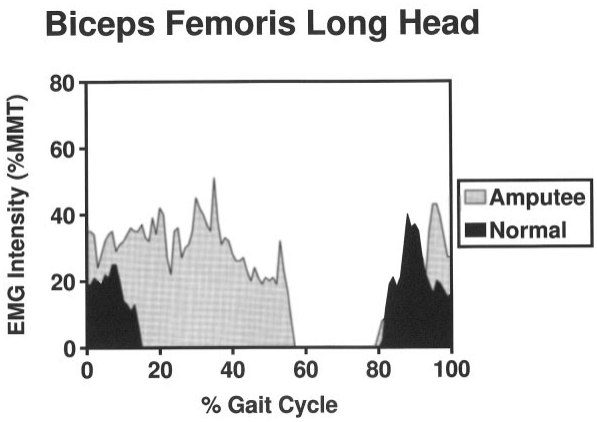


*Figure 1.15. Mean EMG profiles of biceps femoris long head for trans-tibial amputee and control group (% MMT = percentage of maximal muscle test).*

## 1.2 Purpose of this project

Prosthetic walking can be characterised by a reduced moment of force, and the following reduced joints power. A greater muscular activation is an important detail of amputee gait. A co-contraction of agonist and antagonist muscles can be the possible reason of the reduced moments. Therefore, the energy demands are altered substantially by using a prosthesis.

An optimization of the prosthetic assembly is needed and therefore an individualised model should be developed.

The analysis of the kinematics is useful to check if there are asymmetries in the gait cycle of the subjects, while the moments of force and the patterns of mechanical power, that the joint present, are important to understand if the subject is moving in a correct way.

In this study I am going to adopt the same experimental procedures that were used in the previous projects. In this case I take also advantage of AnyBody Modeling System, creating a model suitable for trans-tibial amputees.

This model will help to check the kinetics and biomechanics of amputee gait.

The results that I'll achieve, will be useful to observe if there are asymmetries in the gait of amputees compared with the gait of healthy subjects.

The first goal of this study was the development of a model which accounts for the physical properties of the prosthesis, plus allows to investigate muscle activations during amputee gait.

A greater muscular activity and a reduced moment of force are expected in the amputees subjects, as consequence of a co-contraction of agonist and antagonist muscles (as describes Winter et al. 1988).

The same model can be used for an other purpose of this study.

The second goal of the project is to apply healthy kinematics to the amputee model. This operation is useful to investigate the hypothetical effect of managing to get an amputee walking perfectly symmetric.

# Chapter 2.

# Prosthetic feet used during the data collection

## 2.1 Introduction

Recently prostheses guarantee good performances. In the previous times, amputees used a peg leg as a prosthesis, but it was not able to simulate a normal gait.

As reported Gordon et al. (1960) and Edelstein et al. (1988), prosthetic feet are divided in several groups, and this depends on the movements that they allow.

There is the single-axis, that is the simplest model because of the economy of installation and the maintenance. This kind of prosthesis provides only the plantarflexion and dorsiflexion of the foot. It does not provide inversion and eversion, and it does not absorb a possible torque produced during walking. In the front part of the foot, that adopts the single-axis structure, there is a firm-rubber that limits dorsiflexion. Posteriorly, there is a second rubber part restricting the plantarflexion of the foot.

Another kind of prosthetic foot is characterised by a double-axis ankle. This structure, allows for inversion and eversion of the foot, but not the absorption of the torque caused by walking. The prosthetic foot that permits the absorption of the torque is characterised by a transverse-rotation ankle.

A problem that the double-axis and the transverse-rotation ankles present is due to the maintenance and the frequent repairs. Some functions are common to all the several kind of prosthetic feet: 1) support when the amputee is standing, or during the stance phase of gait; 2) shock absorption at heel strike. The most important requirements that a prosthetic foot should have are the durability, the simple construction of the structure to obviate the need for repairs or replacements. Such a foot should offer sufficient absorbing the shock after the heel strike, and, in the same time, should be light in weight.

## 2.2 S.A.C.H. foot

After the Second World War there were several studies about the development of prostheses, and the evolution of these studies is represented by the S.A.C.H. (Solid Ankle Cushion Heel) prosthetic foot. In this kind of prosthesis the foot and the ankle are combined together with a compressible heel attached to the shank of the leg.

### 2.2.1 Structural characteristics

The structure of the prosthetic foot is characterised by a keel made of wood and a heel of neoprene and sponge rubber. There is also a neoprene toe added to the forward section of the foot. The characteristics of the gait of the amputees are influenced by the installation and the adjustment of the S.A.C.H. foot.

*Figure 2.1. S.A.C.H. foot.*

There is a three-eighths of an inch steel carriage bolt that attaches the foot to the prosthetic shank. A section of wood receives this bolt at the distal end of the shank. The compressibility of the S.A.C.H. foot is the reason why the prosthetic part of the shank should be made one-fourth of an inch longer to compensate for this. The attachment of the foot with the shank is helped and re-enforced by using some glued dowel joints positioned between the keel and the final section of the shank made of wood.

The foot is shaped, especially the heel. The point of the heel is displaced one-fourth of an inch lateral to the mid-line. Without doing this operation, the body weight will be transferred in the lateral side of the heel cushion during the heel contact.

After heel strike, the foot rotates outward about the axis of the leg, so the forward part of the foot moves laterally, while the point of the heel moves medially. Shaping the heel of the foot one-fourth of an inch lateral to the mid-line, the body weight is loaded through the geometric center of the heel after toe-off. This operation of shaping the prosthetic heel should be done checking the individual requirements of the amputee.

The heels that are used for the prosthetic foot can be firm, medium and soft. These different heels are chosen by checking the body weight of the amputee, the type of the amputation, other engineering and medical considerations.

From Figure 2.1 it can be seen that the S.A.C.H. foot shows an elevation of the heel of eleven-sixteenth of an inch (the bottom of the heel is eleven-sixteenth of an inch above the level of the ball of the foot). The S.A.C.H. foot presents several size ranges, and also special sizes and shapes can be realized for women and children.

The first step, before installing the prosthetic foot, is to do some walking trials. The purpose is to find the best configuration of the foot. In some instances is necessary to modify the position of the keel, to limit a possible excessive dorsiflexion of the toe during heel strike.

After these adjustments, the prosthetic foot can be fixed to the shank. Some procedures have to be done after the attachment operation (one-quarter of an inch addiction to the length of the shank) to give the most appropriate length to the shank. The SACH foot provides the plantarflexion and dorsiflexion of the foot, and the absorption of the shock during walking.

The compression of the cushion heel simulates the plantarflexion movement, and it does the important function of absorbing the shock during heel strike. It guarantees a smooth function

during the initial part of the stance phase. The weight is well distributed during the mid-stance phase.

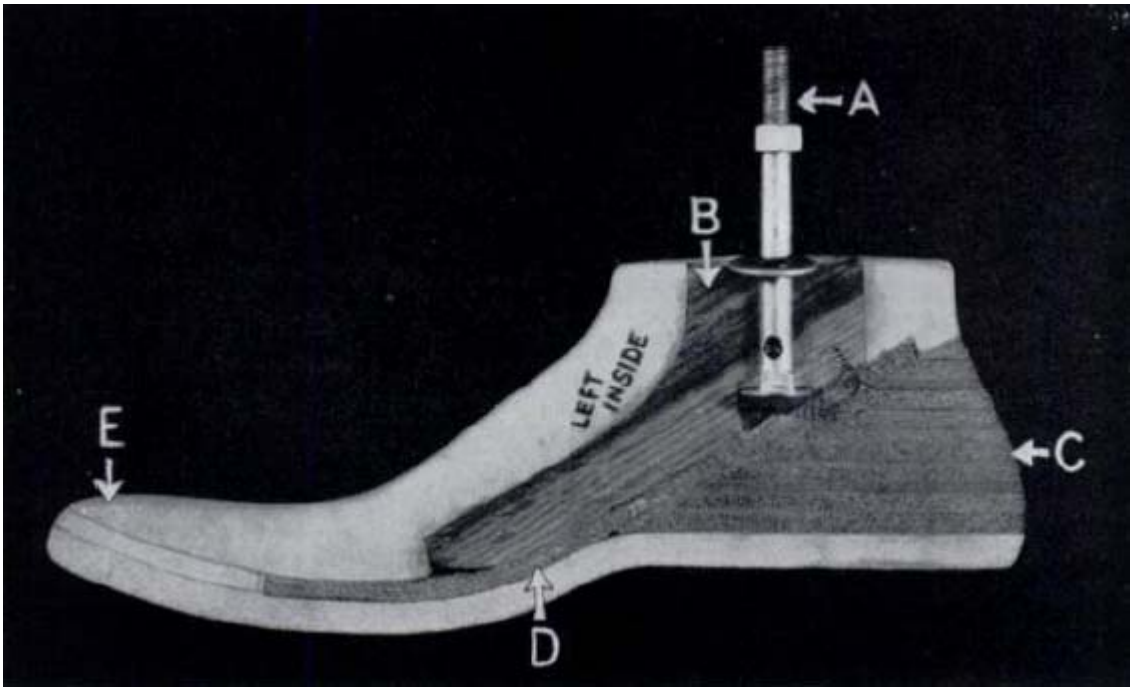


*Figure 2.2. Sagittal section of the S.A.C.H. foot. A=the carriage bolt, three-eighths of an inch in diameter, with the head embedded in the keel; B=wooden keel; C=laminated cushioned rubber heel; D=belting between neoprene outer cover and wooden keel; E=neoprene toe.*

### 2.2.2 Advantages and disadvantages

The most relevant advantages that S.A.C.H. foot provides are the shock absorption at heel strike and the reduced amount of maintenance and repairs, if compared with the previous wooden models of foot. Another important point for the S.A.C.H. foot is the stability that it provides to the amputee during gait. This is permitted by the heel that can be shaped. The amputee feels less fatigue, during walking, by using this kind of prosthesis, and the irritation of the stump is negligible. The maintenance is reduced, and the deterioration is minimal if compared with the previous wooden feet.

A problem that the S.A.C.H. foot presents is given by the compressible heel, that can provide some instability, and this impairs balance when the amputee is standing up, and during the stance phase of gait.

*Table 2.1. S.A.C.H. foot characteristics.*

| Characteristic | 1S90 | | | | | | |
|---|---|---|---|---|---|---|---|
| Mobility Level | 1+2 | | | | | | |
| Heel height | 10 +/- 5 mm | | | | | | |
| Sides | left (L), right (R) | | | | | | |
| Sizes | 22 cm | 23 cm | 24 cm | 25 cm | 26 cm | 27 cm | 28 cm |
| System height 2R54/2R31/2R8 | 55 mm | 58 mm | 61 mm | 64 mm | 67 mm | 70 mm | 72 mm |
| Weight ** (in g) | 300 | 330 | 380 | 420 | 460 | 545 | 635 |
| Max. body weight | 100 kg | | | | 125 kg | | |

## 2.3 Greissinger foot

S.A.C.H. foot is classified as a non articulated assembly, whereas Greissinger foot takes part of the articulated decices. In this category of prosthetic feet there are the single-axis assemblies, that show the simplest structure, where a vertical bolt joins the foot to the prosthetic shank. There is an axle that is perdincular to the bolt and permits the foot to move in the sagittal plane. This device enables dorsiflexion and plantarflexion of the foot. The single-axis, after heel strike, guarantees a plantarflexion that gives stability to the amputee. The plantarflexion bumper can be substituted to increase the stability of the knee. A disadvantage of the single-axis can be the gap between lower and upper portions of the assembly.

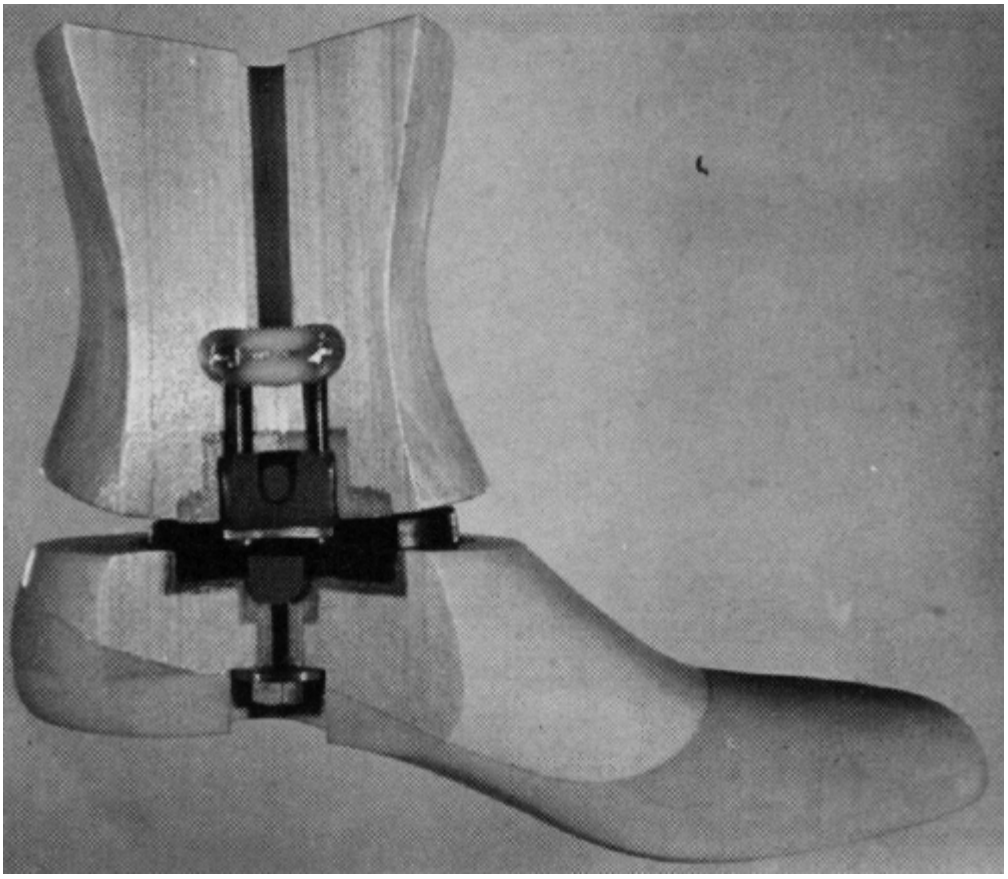

*Figure 2.3. Greissinger foot multiple-axis assembly.*

This kind of device does not reproduce the inversion and eversion of the foot.

There are severeal multi-axis assemblies available that permit for passive motion in the trasverse, frontal and sagittal planes. Greissinger foot is one of these designs.

With multi-axis devices the stress is been absorbed in the trasverse and frontal planes, as well as the sagittal plane. It is preferable to use this kind of assemblies especially when walking on slopes and uneven surfaces. A disadvantage that all the multi-axis devices present is the price, since they are very expensive, the maintenance and the weight.

*Table 2.2. Greissinger foot characteristics.*

| Characteristic | 1A30 | | | | | |
|---|---|---|---|---|---|---|
| Mobility Level | 2 + 3 | | | | | |
| Heel height | 10 +/- 5mm | | | | | |
| Sides | left (L), right (R) | | | | | |
| Sizes | 24 cm | 25 cm | 26 cm | 27 cm | 28 cm | 29 cm |
| System height 2R54/2R31/2R8 | 67 mm | 68 mm | 69 mm | 70 mm | 71 mm | 72 mm |
| Weight ** (in g) | ~ 620 | ~ 670 | ~ 705 | ~ 760 | ~ 810 | ~ 820 |
| Max body weight | 75 kg | | 100 kg | | | |

# Chapter 3.

# Materials and methods

## 3.1 Gait Lab

The data collection took place in a gait laboratory equipped with a VICON 5.2.9 motion system (Oxford Metrics, Oxford, UK) with eight cameras. The disposition of the cameras was circular. By using this disposition of the cameras, it became more simple to acquire the movement of the markers. Furthermore, there was less possibility about occlusions of the markers during the acquisition, so the user could achieve a more reliable result.

*Figure 3.1. VICON cameras.*

In the center of the room there was one force platform (AMTI Multiaxis Force Platforms) that provided the ground reaction forces.

*Figure 3.2. AMTI force platform.*

There were two digital cameras that were connected with the motion capture system. This was a good added point that could help the user during the data analysis. During the data collection also an EMGsystem amplifier MA300 1998 w Harwin backpack, with ten channels, was used. The data were sampled at 1000 Hz.

## 3.2 Subjects

In this study two males with unilateral trans-tibial amputation (in the right side) composed the subject group. These subjects did not need any assistive devices for the ambulation, and did not have vascular diseases. They showed a good stability using their prosthesis, since they fitted it some years ago. One of the two amputees used S.A.C.H. foot, whereas the other one used Greissinger foot. A healthy man was studied, to compare the results with those of amputees. This healty individual served as the control. He did not show any musculoskeletal or neurological impairments, and he was free of any conditions that could affect the gait.
The characteristics (mean) of the subjects can be seen in the following table.

*Table 3.1. Subjects characteristics mean (S.D.).*

| | TTA group (n=2) | Control subject |
|---|---|---|
| Age (y) | 55.5 (14.849) | 67 |
| Eight (m) | 1.82 (0.039) | 1.76 |
| Weight (kg) | 90.4 (9.334) | 83.4 |

## 3.3 Procedures

### 3.3.1 Preparation of the subjects

During the data collection the subjects were using their prosthetic foot (S.A.C.H. foot and Greissinger prosthesis). This was the reason why the TTA group showed a good familiarity with the prosthesis during the gait.

The fitting and alignment procedures followed the prosthetic principles.

### *Anthropometric parameters*

First of all the prosthesis was removed, and weighted (1.321 kg S.A.C.H. foot, 2.4 kg Greissinger prosthesis).

After that operation, lower extremity anthropometric measurements parameters were made on all subjects.

*Table 3.2. Anthropometric parameters.*

| **Anthropometric parameter** | | |
|---|---|---|
| Body mass | Left Elbow Width | Right Shank Rotation |
| Height | Right Elbow Width | Left Static Plantarflexion |
| Left Leg Length | Left Wrist Width | Right Static Plantarflexion |
| Right Leg Length | Right Wrist Width | Left Static RotOff |
| Left Knee Width | Left Hand Thickness | Right Static RotOff |
| Right Knee Width | Right Hand Thickness | Left Ankle Abduction/Adduction |
| Left Ankle Width | Left ASIS Trocanter Distance | Right Ankle Abduction/Adduction |
| Right Ankle Width | Right ASIS Trocanter Distance | Head Offset |
| Inter ASIS Distance | Left Thigh Rotation | |
| Left Shoulder Offset | Right Thigh Rotation | |
| Right Shoulder Offset | Left Shank Rotation | |

### 3.3.2 Data collection

Three-dimensional data of 27 markers were collected using an eight cameras VICON 5.2.9 motion system (Oxford Metrics, Oxford, UK). The marker-set was based on the Plug-in marker placement protocol.

*Table 3.3. Marker label, description and position (only left side markers are listed, the positioning of the right side is identical).*

| Number | Label | Description | Position |
|---|---|---|---|
| 1 | LFHD | Left front head | Located approximately over the left temple |
| 2 | RFHD | Right front head | Located approximately over the right temple |
| 3 | LBHD | Left back head | Placed on the back of the head,roughly in a horizontal plane of the front head markers |
| 4 | RBHD | Right back head | Placed on the back of the head, roughly in a horizontal plane of the front head markers |
| 5 | C7 | 7th Cervical Vertebrae | Spinous process of the 7th cervical vertebrae |
| 6 | T10 | 10th Thoracic Vertebrae | Spinous Process of the 10th thoracic vertebrae |
| 7 | CLAV | Clavicle | Jugular Notch where the clavicles meet the sternum |
| 8 | STRN | Sternum | Xiphoid process of the Sternum |
| 9 | RBAK | Right Back | Placed in the middle of the right scapula. This marker has no symmetrical marker on the left side. This asymmetry helps the auto-labeling routine determine right from left on the subject. |
| 10 | LSHO | Left shoulder marker | Placed on the Acromio-clavicular joint |
| 11 | LUPA | Left upper arm marker | Placed on the upper arm between the elbow and shoulder markers. Should be placed asymmetrically with RUPA |
| 12 | LELB | Left elbow | Placed on lateral epicondyle approximating elbow joint axis |
| 13 | LFRA | Left forearm marker | Placed on the lower arm between the wrist and elbow markers. Should be placed asymmetrically with RFRA |
| 14 | LWRA | Left wrist marker A | Left wrist bar thumb side |
| 15 | LWRB | Left wrist marker B | Left wrist bar pinkie side |
| 16 | LFIN | Left fingers | Actually placed on the dorsum of the hand just below the head of the second metacarpal |
| 17 | LASI | Left ASIS | Placed directly over the left anterior superior iliac spine |
| 18 | RASI | Right ASIS | Placed directly over the right anterior superior iliac spine |
| 19 | LPSI | Left PSIS | Placed directly over the left posterior superior iliac spine |
| 20 | RPSI | Right PSIS | Placed directly over the right posterior superior iliac spine |
| 21 | SACR | Sacral wand marker | Placed on the skin mid-way between the posterior superior iliac spines (PSIS). An alternative to LPSI and RPSI. |
| 22 | LKNE | Left knee | Placed on the lateral epicondyle of the left knee |
| 23 | LTHI | Left thigh | Place the marker over the lower lateral 1/3 surface of the thigh, just below the swing of the hand, although the height is not critical. |
| 24 | LANK | Left ankle | Placed on the lateral malleolus along an imaginary line that passes through the transmalleolar axis |
| 25 | LTIB | Left tibial wand marker | Similar to the thigh markers, these are placed over the lower 1/3 of the shank to determine the alignment of the ankle flexion axis |
| 26 | LTOE | Left toe | Placed over the second metatarsal head, on the mid-foot side |

| | | | |
|---|---|---|---|
| 27 | LHEE | Left heel | of the equinus break between fore-foot and mid-foot<br>Placed on the calcaneous at the same height above the plantar surface of the foot as the toe marker |

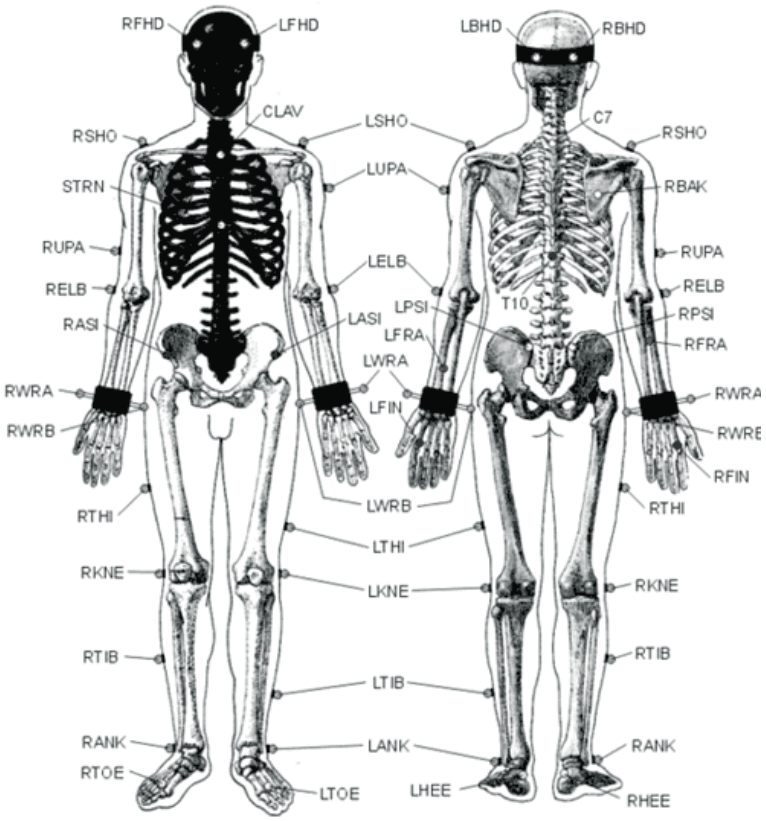


*Figure 3.3. Plug-in marker placement protocol.*

The motion data were sampled at 100 Hz, and filtered using a Woltring filter parameter set to 20. The procedure explained by Giakas et al. (1997) was used.

Ground reaction forces were recorded from a AMTI force plate 508 x 468 mm (Advanced Mechanical Technology, Watertown, MA) concealed in the middle of a 10 m walkway. The force plate data were sampled at 1000 Hz.

To record the muscular activity, electrodes were applied by adhesive tape at the level of the muscle bellies.

The following muscles were analyzed:

1. Tibialis anterior (only left side);
2. Gluteus maximus;
3. Gastrocnemius lateralis (only left side);
4. Vastus lateralis;
5. Vastus medialis;
6. Biceps femoris;

Subjects were instructed to walk in a natural way, at a free walking velocity along the 10 m walkway.

A trial was considered successful if the subject land the foot of interest on the force platform.

Motion, force plate and EMG data were collected simultaneously.

## 3.4 Data analysis

### 3.4.1 Procedure to achieve the results

In the end of the folder InverseDynamicStudy, that is located in the file named *GaitLower-Extremity.main.any*, there is the possibility to include a file called *GCDOutput.any*.

In this file it can be seen that there is the definition of a AnyOutputGCD structure.

This is useful to create a data file on the GCD (Gait Cycle Data) format.

The advantage that can be achieved by including this file is that all the variables included in it will be converted in a *.gcd* file, and they can be checked by using MATLAB, or MlsViewer.

The first purpose of this study is to compare the gait of amputees with the gait of sound people. To do this, joint angles, joint moments, power, muscular activity, and ground reaction forces are studied.

It can be seen that in the first part of the AnyOutputGCD object there is the definition of the events that are going to define the gait cycle of the model.

Two gait cycles will be separately defined by using the time specifications LeftHeelStrike1 and LeftHeelStrike2 for the left side, RightHeelStrike1 and RightHeelStrike2 for the right side.

The events are taken from the C3DFileData folder.

After the definition of the events, there are two pre-defined folders named Left and Right. In both of them there are the outputs that are obviously related to the relative side.

In these folders are already included the activity of several muscles, joint angles, joint reaction forces and joint moments.

The angles that will be observed are:

- Knee Flexion/Extension;
- Hip Flexion/Extension;
- Hip Abduction/Adduction;

The moments of the joints that will be studied are:

- Knee Flexion Moment;
- Hip Flexion Moment;
- Hip Abduction Moment;

To calculate the power of the joints the same formula of the previous studies is used:

$P_j = M_j \cdot \omega_j$,

where it becomes obvious that the power is the result of the multiplication between the moment of the joint ($M_j$) and the angular velocity ($\omega_j$).

To study the muscular activity of the lower limbs, the following muscles are included in the file named GCDOutput.any:

- Vastus Lateralis and Medialis;
- Gluteus Maximus Superior;
- Biceps Femoris;

In the main file an AnyOutputGCD class template is included. This object will contain the variables related to the ground reaction forces (vertical, anterior-posterior and medial-lateral components).

### 3.4.2 Selection of the events

For the calculation of the joint angles, the events that LeftHeelStrike1 and LeftHeelStrike2 (for the left side), RightHeelStrike1 and RightHeelStrike2 (for the right side) are considered.

The procedure useful to calculate joint moments, power, muscular activity, and ground reaction forces, is different. The point is that to calculate the joint moments (and therefore the power) the ground reaction forces are needed. For this reason HeelStrike and ToeOff that include the period of time when the foot of the model is touching the force plate needes to be selected.
After this operation the graphs that represent the joint angles (100% of the gait cycle), and the graphs that show the moment and power of the joints, the activity of the muscles, and the ground reaction forces (only the stance phase, 60% of the gait cycle) will be observed.

### 3.4.3 Development of *virtual amputee*

In this paragraph the procedure to apply healthy kinematics to the amputee model is described.
First of all, the MotionAndParameterOptimizationSequence needes to be done by using the c3d file from the amputee data collection. The results are several output files (optimized parameters, and euler angles) that will be used during the InverseDynamic analysis sequence.
The same procedure has to be followed for the data collection from the normal subject.
The optimized parameters from the amputee trials and the other several outputs (that include the kinematics) from the healthy trials will be used.
The file named TrialSpecficData.any (that is located in the GaitLowerExtremity folder) contains the name of the “healthy” c3d file, so the ground reaction forces are calculated from the healthy data collection.

## Chapter 4.

# Inverse dynamics

### 4.1 Forward and Inverse Dynamic

The musculoskeletal system is assumed to be a rigid-body system, so standard methods of multibody dynamics can be applied. The main problem is that the number of muscles available to move the segments is larger than the degrees of freedom of the mechanical system, more then what is needed to drive the degrees of freedom that characterize the system.

As Damsgaard et al. (2006) observed, having such a model there are two different kinds of approach possible which are forward and inverse dynamics.

With forward dynamics the motion is been computed starting from a predicted muscular activation. This approach is very useful to check the detailed modelling of various physical phenomena, but the problem is the optimization cost that the model requires to perform a specific task.

In the case of an inverse dynamics study the muscle activation starting from a known motion computed. The consequence is that there are a lot of restrictions on the model, but in this case the optimization cost is less than in the forward dynamics case. This is the reason why with inverse dynamics models of higher complexity and models including a greater number of muscles can be generated.

### 4.2 Muscle recruitment

The solution of the muscle recruitment problem in the approach of inverse dynamics is given by a optimization problem that can be generally presented in the following form:

$$Minimize_{\,f}\ G(\underline{f}^{(M)}) \tag{1}$$

Subject to $\underline{C} \cdot \underline{f} = \underline{d}$, (2)

$$0 \le f_i^{(M)} \le N_i, \quad i \in \{1,...,n^{(M)}\}, \tag{3}$$

where G is the objective function, and it is minimized with respect to all unknown forces in the problem. These forces are represented by the form $f = \left[ f^{(M)T} \; f^{(R)T} \right]^T$, where $f^{(M)}$ are the muscle forces, and $f^{(R)}$ are the joint reaction forces.

Equation (2) represents the dynamic equilibrium equations, where $\underline{C}$ is the coefficient-matrix for the unknown forces and the right-hand side. $\underline{d}$ represents all the applied loads and inertia forces.

It can be seen from equation (3) that the constraints on the muscle forces are non-negative. This is in reflection that muscles can only pull, not push, and $N_i$ is the strength of each individual muscle.

There are some forms of the $G$ objective function, the *polynomial criteria* (4), and the *soft saturation criteria* (5).

$$G\left(\underline{f}^{(M)}\right) = \sum_{i=1}^{n^{(M)}} \left( \frac{f_i^{(M)}}{N_i} \right)^p, \tag{4}$$

$$G\left(\underline{f}^{(M)}\right) = -\sum_{i=1}^{n^{(M)}} \sqrt[p]{\left(1 - \frac{f_i^{(M)}}{N_i}\right)^p}, \tag{5}$$

where it can be seen that there are a power variable and a normalizing function for each muscle, $N_i$.The normalized muscle force is often called *muscle activity*. $N_i$ can be chosen measuring the strength of the muscle, which might be considered a realistic assumption from a physiological point of view.

Another possibility that can be used to find the expression of $G$ is the min/max formulation, that presents the following form

$$G\left(\underline{f}^{(M)}\right) = \max\left( \frac{f_i^{(M)}}{N_i} \right), \tag{6}$$

that is the minimization of the maximal muscle activity.

This criterion, if it is compared with the two previous, can be transformed into a linear problem, which makes it numerically efficient and possible to solve with a finite algorithm. It is generally agreed that, considering the (4) and (5) expressions of $G$, if $p = 1$ the achievable result is

physiologically unreasonable, namely that the stronger muscles do all the work while it is known for real muscles to share the loads whenever possible.

When the value of $p$ starts to increase the (4) and (5) expressions of $G$ become less numerically attractive. The soft saturation criteria can cause numerical problems when activities are close to the upper limit, while the min/max criterion utilizes the muscles optimally. In this case the activities do not exceed the limit before becoming unavoidable. This criterion is attractive from a numerical and a physiological points of view.

If it is assumed that muscle fatigue and activity are proportional, the criterion postpones the fatigue as much as possible. This criterion that minimizes the fatigue is the foundation of the inverse dynamic analysis in the AnyBody software.

## 4.3 AnyBody Modeling System

The AnyBody Modeling System allows to set up such a musculoskeletal model.

This software is designed to meet four goals:

1. to be a modeling system. The users should be able to create a new model starting from scratch or use (or modify) the models already created to suit different purposes;
2. to facilitate model exchange and cooperation on model development;
3. to have sufficient numerical efficiency to allow optimization on inexpensive computers;
4. to be capable of handling body models with a realistic level of complexity.

The software is characterized by two applications, a Window graphical user interface (GUI) and a console application. Both of them have the same modelling facilities, but they differ in the ways they can be used.

AnyBody Modeling System is based on a text-based input. A modeling language has been created, and it is named AnyScript. In this case a text-based input is very useful because it is easy to develop and maintain. After this, the first two points described before require a versatile and flexible input to be achieved.

### 4.3.1 AnyScript modeling language

To develop multibody dynamics models is good to use a declarative, object-oriented language like AnyScript. It is divided into two sections:

1. the model section that contains the definition of the mechanical system, the body and the boundary conditions;
2. the study section contains the list of operations written by the user. These are the procedures that the model has to do, and they can be performed by the software.

AnyScript is a declarative language, and this means that it has a list of predefined classes, and the user can create objects starting from these classes. In this list there are basic data types (numbers, strings), mechanical objects types (segments, joints, drivers, forces, muscles) and operational and model management classes.

By using this modeling language, the operator can not use code like “do” loops and “if-then-else” .

The study section, that was described before, is very useful because the user can apply several operations to be performed on the model. For example, kinematical analysis, kinetic analysis, muscle calibration and systematic parameter variations.

The operation created by the user can refer to entire model, or only to some sections of the model.

*Figure 4.1. Example of a full body model.*

An important advantage that the AnyScript modeling language shows is that whenever a new "operation" or "study" is implemented in the data structure, it is available also in the interfaces of the software.

The organization of this structure allows to create models such as the full body model that is represented in Figure 4.1.

The user, using the AnyScript language, is able to create a tree structure, similar to a file system. Folders can contain specific parts of the model, and the operator can exploit references to different sections of the model. In this way the model can be built by several operators working of different files, and models. If, for instance, one user is working on an arm model, and another user is working on the hand model, it is very difficult to combine these models together. To make more simple this operation the structure of the model is been split into two different parts: the body model and the application model.

The first section contains all the parts of the body (segments, joints, muscles and other anatomical data) and several functions related to those (setups for calibrating parameters of the body model). For instance, the muscles parameters need adjustment for given body anthropometrics.

The "application model" section is related to the movements, loads and external objects (tools, bicycles) that characterize the model.

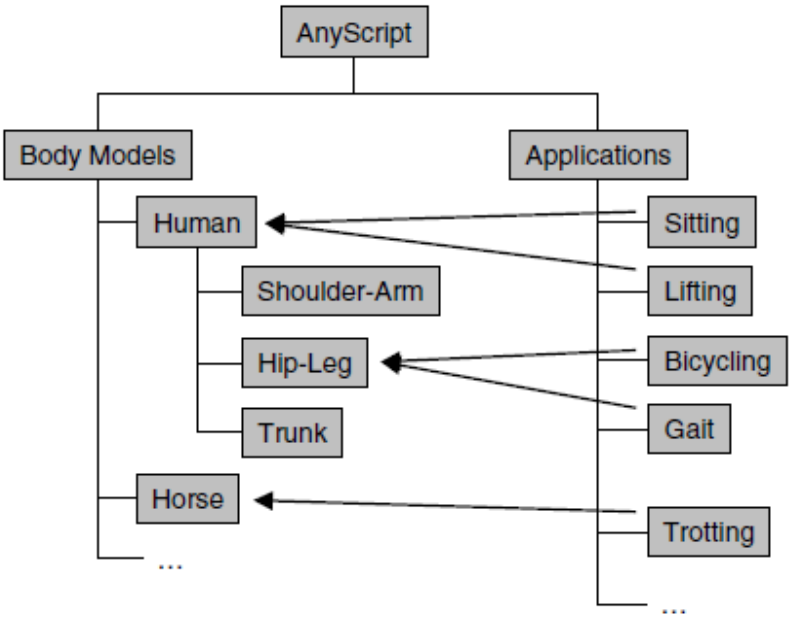


*Figure 4.2.Tree structure that shows the grouping of the models.*

The user can exchange body models and connect them with different types of applications.

From the Figure 4.2 it can be derived that the body model is divided into parts, such that different users can build models of different parts of the body and put them together.

It is difficult to handle the elements that cross the interface between two body models or between the body model and the application. By using AnyScript language, the operator can add the necessary elements outside the basic objects declaration.

If, for instance, there is one operator that is developing a hand model, and another user that is going to create the arm model. How can the first one be sure that his colleague has provided muscle attachment points on the arm for the muscle spanning wrist? In this case, the hand model can contain the necessary additions to the arm model to make the parts compatible.

Figure 4.3 is the example that can explain the structure of the body model repository. It can be seen that the two bicycle-rider models represent identical applications that are combined with a simple 2-D lower extremity, and a more complex 3-D lower extremity.

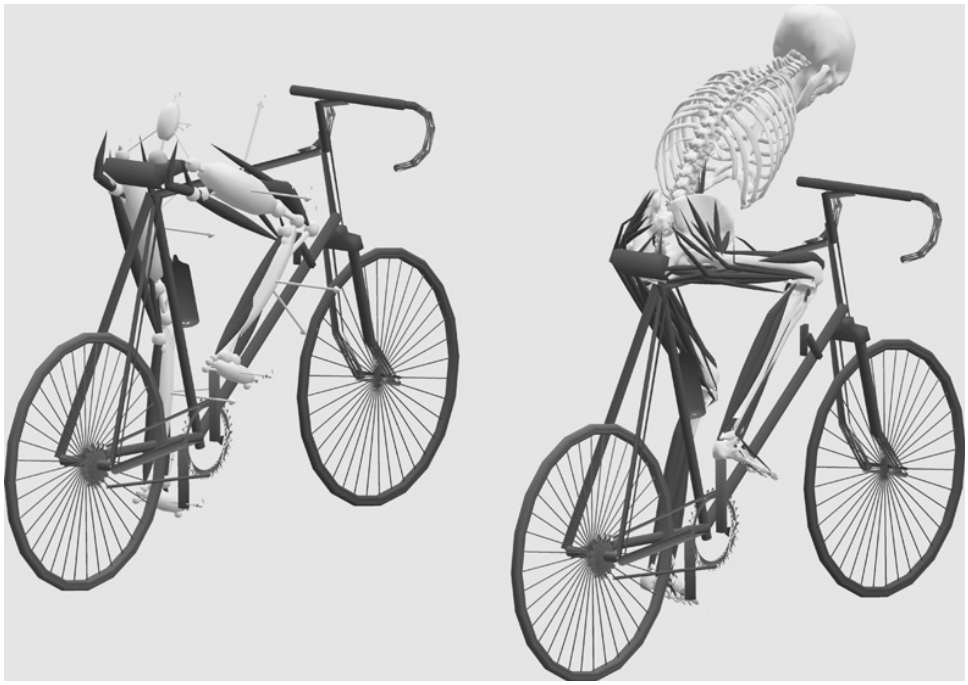

*Figure 4.3. Example of a structured model. The two bicycles are identical applications, and are combined with a 2D lower extremity (left), and a 3D lower extremity (right).*

# Chapter 5.

# Development of the model

## 5.1 Repository

In the *ammrv1.2* repository there are several folders that contain files (*.any*) useful for different purposes. The operator can create a new blank main file, or he can work on the models already created.
The aim of this project is to observe and study the gait of sound and amputee subjects, so the proper folder of the repository to work on is the *GaitLowerExtremity*.

### 5.1.1 GaitLowerExtremity characteristics

From the file *GaitLowerExtremity.main.any* it can be seen that the main is divided into two parts.
The first one that allows the optimization of motion and parameters of the model from the data acquired in the gait lab.
This optimization is based on a method that is useful for the identification of biomechanically parameters in kinematically determinate and over-determinate system from a given motion. The explanation of this method is explained by Andersen MS et al. (2009).
The second one is useful to load the *InverseDynamicAnalysisSequence*, that generates the final results (movements of the joints, strength of the muscles, and the outputs decided by the operator).

```
//Set this to 1 if you want to run the motion and Parameter
//Optimization identification
//************************************************
#define MotionAndParameterOptimizationModel 1

//Set this to 1 if you want to run the inverse dynamic analysis
#define InverseDynamicModel 0
//Usually only have one of the two switches active so set the
//inactive analysis to 0
//************************************************
```

*Figure 5.1. First part of the code of GaitLowerExtremity.any file. The operator can chose to run the MotionAndParameterOptimizationModel, or the InverseDynamicModel.*

It can be seen that in the main file are included several *.any* files, like BodyPartsSetup2.any (in the *MotionAndParametersOptimizationModel* part) and BodyPartsSetup.any (in the section dedicated to *InverseDynamic*). To include an *.any* file in the main only the name of the file preceded by the formula "#include" needs to be inserted.

The files BodyPartsSetup.any and BodyPartsSetup2.any include the definitions of the segments and muscles that are going to create the musculoskeletal model. In particular, it can be seen the presence of two different kinds of muscles for the TD leg (that is the type of leg that will be used in this project): LEG_TD_MUS_3E and LEG_TD_SIMPLE_MUSCLES. One of them needs to be defined (or none, but not both). In the optimization of the parameters the presence of the muscles in the model is not required, such that in the file BodyPartsSetup2.any only the segments of trunk, right leg TD, and left leg TD are defined. For the InverseDynamic study the user can decide to include the muscles in the model. Initially the one using the simple muscles of the TD legs was used.

Another important file that is included in the *GaitLowerExtremity.main.any* file is *ModelSetup.any*. In this file all the markers of the model are defined. It can be seen that every marker has name, placement, optimization, weight, and the position (that is the center of a local coordinates system).

The optimization can be done along the axes of the local coordinates system that allow this operation. This happens if the value is turned to "On". When loading the main file, it becomes obvious that (by opening the Model View) the markers of the model are represented with a small coordinates system where its axes are green if the optimization is allowed in that direction, or red if the optimization is not allowed (Figure 5.2).

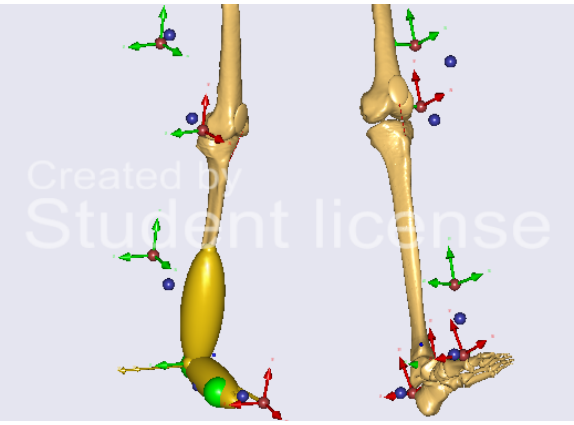


*Figure 5.2. Example of a lower extremity model. The blue markers are those from the c3d file, while the red ones are the markers of the model.*

The weight of the markers is an index that shows the importance of the markers. Weight functions can usually be used to put more emphasis on the kinematic constraints equations then on others. This will force the motion of the model closer to the constraints with the higher weight. There are two occasions when weight function can be very useful: 1) Depending on the placement of the markers (likely skin movement artifacts) one kinematic constraint can be weighted higher than another; 2) For example, if a marker temporarily dropping out of sight of the cameras a temporarily weight of zero can be assigned. This will eliminate the marker from the model in the interval where it is invalid.

It can be seen that an *AnyInputC3D* property is defined at the beginning of the ModelSetup.any. This is the file which contains all the information about the data collection that is included in the analysis. This information is obtained from the motion capture system, the marker-set used during the acquisition, the ground reaction forces from the force platforms, the EMG.

To see the results of the optimization the markers are setted to “On” in the *ConstructModelOnOff*. The markers from the c3d file will be displayed, but the analysis time will be much slower. After the optimization of the parameters it becomes obvious that the markers of the model are very close to the blue markers which represent the position of the optical markers from the c3d file.

At the beginning of the file named *TrialsSpecificData.any*, the default c3d file name was replaced with the name of the to be analyzed. It can be seen that in this file there is an *AnyFolder* called Anthropometrics where there are all the anthropometric parameters of the subjects (body mass,

height, length of the body segments). After this, there is a folder named *InitialPositionOfBody*. Here initial positions of the body segments can be changed. Sometimes it is necessary to modify those values to run the InitialPosition operation and to make more simple and fast the optimization. Further, a file that is included in the main *GaitLowerExtremity.main.any* is the *Environment-AutoDetection.any*. In this file there is the definition of the force platforms that are used during the data collection. One element that marks the platform is the type. The default value is Type4. For the kind of platform that is going to be used during the acquisitions, it's better to use another type of platform named Type2, and it is defined in the new repository.

## 5.2 Generation of an individualized leg-stump model

### 5.2.1 Generation of the "LegTD_Amputee" folder

The first operation that is done for this study is to create a copy of the folder LegTD, called LegTD_Amputee. This is useful because it is needed to represent the amputation only in one limb. It is worked on the sound leg using the LegTD folder (the original one), and the folder named LegTD_Amputee is created to work on the amputee limb.

This folder, that contains the same files that are in the original one, is located in directory named AAU Human. This folder contains all the components of the "body" of the model, and several functions related to it. Further details on the information contained in this folder will be explained below, when describing the proceedures to generate the final model.

#### 5.2.1.1 Removal of foot and talus

After this operation the foot and the talus are removed from the model. To do this the folders called Talus and Foot in the *Seg.any* (the file where all the segments of the model are defined) are excluded. With that, there are two *Seg.any* files, the original one (of the sound limb), and the amputee one (of the limb that shows the amputation). This is a workable solution to study trans-tibial unilateral amputees. Subsequently, all the muscles that are in the foot and in the tibia are removed from the model, as these are not existent in the amputee.

When loading the *MotionAndParametersOptimizationModel* it can be seen in the view window that the skeleton appears without the foot and the talus.

#### 5.2.1.2 Removal of the lower part of the tibia

As the next step, the lower part of the tibia needes to be removed. For this purpose a CAD software named MeshLab is used, that is useful to process and edit unstructured 3D triangular meshes.
This software allows to generate and edit *.stl* files, which contain surface geometry and can be converted in to *.anysurf* format using an AnySurf translator. This operation is used for the design of the altered limb model.
Starting from a file that represents a sound tibia, with the operation *Select faces in a rectangular region* the parts of the limb that need to be removed are selected.

*Figure 5.3. Example of a tibia. The red part is selected, and it's going to be removed.*

*Figure 5.4. Example of tibia. The distal part of the tibia is been removed.*

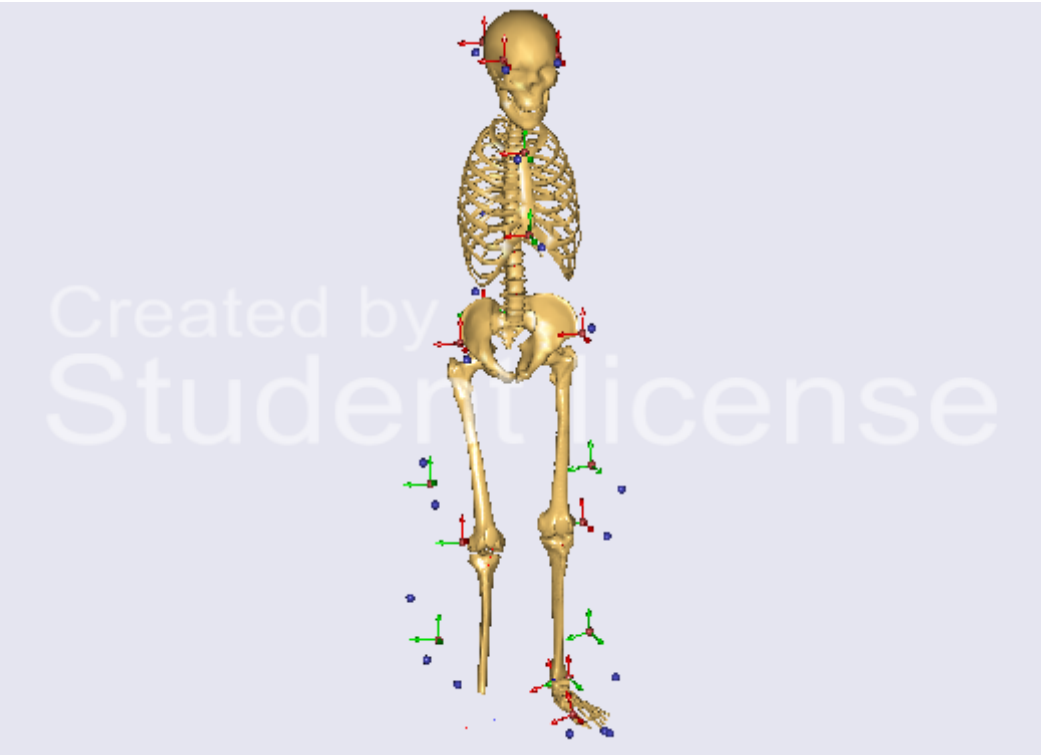


*Figure 5.5. Skeleton model with the lower part of the tibia that is cut.*

#### 5.2.1.3 Other changes

There are several other changes needed, especially on the files in the folder LegTD_Amputee. Initially the references from the file named InitialPosition.any to the foot and the talus have to be removed.

In the file Interface.any it can be seen that there are two folders related to the plantarflexion and the eversion of the ankle. Consequently, the references to ankle, talus and foot are excluded from these two folders.

After this operation, the last lines of this *.any* file need to be removed. They are “pointers” to the HeelNode, ToeMedialNode and ToeLateralNode. Without these points there are some errors because of the failed detection done by the force platform. A copy of the HeelNode and the ToeLateralNode needs to be created in my prosthesis model, which are also used to recognize the events of heel-strike and toe-off, that are very important in gait cycle analysis.

Further, in the file Jnt.any there are two *AnyRevoluteJoint* named Ankle and SubTalar which need to be removed.

In the file named JointMuscles.any the *AnyFolders* called AnkleJnt, AnkleEversion, SubTalarEversion are outcommented to exclude them from the calculations.

In Leg.root.any file there is a summation that represents the mass of the leg. In this summation the mass of the foot needes to be removed.

The file named LegMoment.any contains all the calculations of the moments of the body segments. The sections of this file that are referred to the ankle and the talus need to be removed.

In the file LegSimpleMuscles.any the AnyRevoluteJoint named Ankle is excluded, and the *AnyVar* Mass, in the folder named MassSummation, needes to be modified by removing the mass of the foot. The same operations are necessary in the other several files LegNoMuscles.any and Leg3EMuscles.any.

In the file named MannequinValuesFromModel.any the variables AnyVar_AnklePlantarFlexion and AnyVar_AnkleEversion need to be removed.

It can be seen that all the muscles of my model are defined in the file Mus.any. The muscles in the shank of the patients are lacked. All the muscles with insertion or origin in the sections that were removed (foot, talus, lower part of the tibia) need to be excluded.

It can be seen that in the file RightLegMuscles3ESelectedOutput.any are defined several variables that are related to some reaction forces. Those relative to the ankle and subtalar joints need to be removed.

### *GenericBodyModel*

After all these operations, folders named BodyModels and GenericBodyModel are selected. A copy of the files that define the right leg TD needs to be created. There are three versions: RightLegTDMus_3E_Amputee.any, RightLegTDNoMuscles_Amputee.any and RightLegTD-SimpleMuscles_Amputee.any.

In this case, only the file named RightLegTDSimpleMuscles_Amputee is going to be used, but the changes are the same in the other files. The most important operation to do is to replace the reference to the LegTD with the reference to LegTD_Amputee.

```
Right = {

  AnyFolder Leg = {

    #include "..\..\LegTD_Amputee\LegNoMuscles.root.any"

    //Reference to folder which contains the interface
of the right side
      AnyFolder &InterfaceFolder =..Interface.Right;

      //Reference to mannequin value from model folder
      AnyFolder &MannequinValuesFolder =
..MannequinValuesFromModel.AnyFolder_Posture.AnyFolder_Right;
```

*Figure 5.6. Reference to the LegTD_Amputee folder.*

## 5.3 Generation of the “Prosthesis” folder

### 5.3.1 Prosthetic shank

The purpose is to create a joint that allows for plantarflexion and dorsiflexion.

I start by creating a reference to the Seg folder that can be found following the path HumanModel-BodyModel-Right-Leg-Seg.

The symbol “&” in front of the local name means that *ref* is a reference (a pointer) to HumanModel.BodyModel.Right.Leg.Seg rather than a copy of it.

The folder *ref* contains the prosthetic segments that I’m going to describe. An *AnySeg* needs to be created by including the template from the Classes tab in the left hand side of the editor window.

The name of the new segment, the Prosthetic_Shank, its mass and its inertial properties are inserted here. Obviously, Jii is a vector, but not a 3 X 3 matrix. The reason is that Jii contains only the diagonal members (principal moments of inertia), which is all which is needed to specify if the segment-fixed reference frame is aligned with the principal axes. If this condition does not apply, the elements that are not in the diagonal (the deviation moments) can be specified in a property called Jij, which in AnyBody by default contains zeros.

It can be seen that the first two lines of the *Prosthetic_Shank* are commented out. The property r0 and Axes0 respectively represent the initial position and the orientation of the segment in the global coordinates system. The first of these is a simple vector, where the three-dimensional coordinates of the segment in space can be specified. The Axes0 property is a rotation matrix, which specifies the segment orientation. AnyScript has a useful standard function, which can be used for this purpose, and it is named *RotMat*. This function returns a rotation matrix corresponding to a given axis and rotation angle.

These two lines remain uncommented because I have to change the initial position of my prosthesis, so that the “InitialConditions” of the model can run. If the prosthesis is too far from the markers that I have from the c3d file, the optimization may not be able to finish successfully.

```
ref =
{
  AnySeg Prosthetic_Shank =
  {
    r0 = {0.365, -1.7, 0.12};
    //rDot0 = {0, 0, 0};
    Axes0 = RotMat(90*pi/180,z)*RotMat(90*pi/180,x)*RotMat(-20*pi/180,z);
    //omega0 = {0, 0, 0};
    Mass = 2;
    Jii = {0.005, 0.001, 0.005};
    //Jij = {0, 0, 0};
    sCoM = {0, 0.1, 0};
    JaboutCoMOnOff = On;
```

*Figure 5.7. Prosthetic shank.*

The property sCoM represents the position of the center of mass of the segment.

Subsequently, there is the definition of the *AnyRefNode* named ScalingNode, that is a reference frame rigidly attached to another one. The position and the orientation of this frame are specified relatively to its owner/parent node and the angular velocity and acceleration of the node are the same as the owner's/parent's.

After ScalingNode (that is used for the scaling of the segment which is referred) another *AnyRefNode* is defined. It's the prosthetic_shank_attachment, and it's useful to link the prosthesis with the sound part of the shank.

There is, after the prosthetic_shank_attachment, the node that connects the prosthetic shank with the prosthetic ankle. It was named prosthetic_shankankle_attachment, and will be later used to define the joint that will replace the sound ankle. An *AnyFunTransform3DIdentity* named Scale, that is a transformation function, returns a vector equal to the input argument. Finally, the *AnyDrawSeg* is added to draw the segment will be inserted.

### 5.3.2 Prosthetic foot

For the generation of the prosthetic foot model a new *AnySeg* named Prosthetic_Foot is defined. As before, the default properties r0 and Axes0 are commented out, but the initial position of this assignment may need to be edited to enable the operation *InitialCondition* running properly. Mass

and inertia values for this segment are added and another *AnyRefNode* named ScalingNode and an *AnyFunTransform3DIdentity* named Scale are inserted.
A *AnyRefNode* called prosthetic_foot_attachment is added, placed in the prosthetic ankle joint at the node, that was described before, and was named prosthetic_shankankle_attachment.

### *"Prosthetic" heel and toe*

It is necessary to create two *AnyRefNode* more, because the force platform needs a point of reference for the first contact of the foot (Heel) and the last moment of contact of the foot (Toe lateral).
That is why two *AnyRefNodes* named HeelContactNodeLow and ToeLateralContactNode are inserted as well. The operation *AnyDrawSeg* is added to generate a graphical representation of the prosthetic foot.

### 5.3.3 Generation of the joints

#### 5.3.3.1 Connection sound shank-prosthetic shank

First of all the prosthetic shank should be fixed with the sound part of the shank. A reference to the folder named *Jnt* (where are defined all the joints of the model) is written. This reference, that is called refRightJnt, contains two joints.
The first one is named Prosthetic_Shank_Jnt, and it is a standard joint. By studying the AnyScript reference manual it becomes obvious that an AnyStdJnt is a function that creates a rigid joint, i.e., it describes a fully constrained rigid-body motion.
Between the brackets the two *AnyRefFrame* are included. These are the reference frames that are going to be joined. It is important to notice that at least one of them has to be movable. The first frame is referred to the prosthetic_shank_attachment, and the second one is referred to the shank_attachment, that is an *AnyRefNode* defined in the reference called refRightShank.

#### 5.3.3.2 Prosthetic ankle

After the definition of the AnyStdJoint named Prosthetic_Shank_Jnt, the joint that will represent the prosthetic ankle is created.

The suitable object that should be created in this case is the AnyRevoluteJoint, that is an ideal hinge that allows the rotation about one axis.

The two reference frames that are going to be joined are the prosthetic_foot_attachment and the prosthetic_shankankle_attachment.

The prosthesis is been created. From Figure 5.8 it can be seen that the prosthesis is attached to the sound part of the tibia.

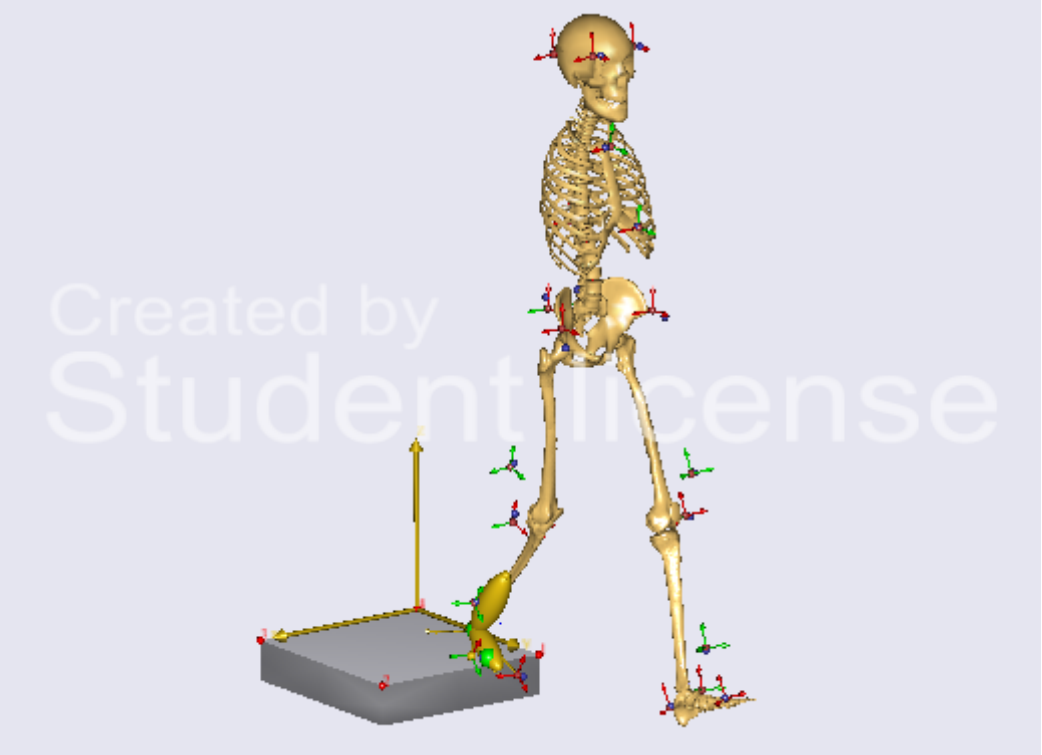


*Figure 5.8. Amputee model view.*

# Chapter 6.

# Results

## 6.1 Stride characteristics

The first amputee shows the slowest velocity (1 m/s for both sides), whereas the second amputee is faster also than the normal subject (1.79 and 1.78 m/s vs. 1.56 and 1.58 m/s respectively in the left and right side).

Amputee 1 demonstrates a reduced stride length compared with the normal subject (0.61 vs. 0.80 m in the left side, 0.67 vs. 0.81 m in the right side).

Amputee 2 presents a greater stride length using the sound limb than the amputee side (0.92 vs. 0.83 m).

The amputee group shows a long stance phase using the sound limb (68.5% and 62.1% of the gait cycle respectively for amputee 1 and 2 in the left side, while in the right side the percentages are 61.8% and 60.4% of the gait cycle).

*Table 6.1. Stride characteristics (S.D.)*

| **Amputee 1** | | |
|---|---|---|
| | **left** | **right** |
| Velocity (m/s) | 1.00 (± 0.016) | 1.00 (± 0.026) |
| Cadence (steps/min) | 93.6 (± 1.41) | 93.9 (± 2.59) |
| Stride length (m) | 0.61 (± 0.021) | 0.67 (± 0.023) |
| Stance phase (% GC) | 68.5 (± 1.87) | 61.8 (± 2.08) |
| Single support phase (% GC) | 38.2 (± 1.69) | 31.7 (± 2.56) |
| **Amputee 2** | | |
| | **left** | **right** |
| Velocity (m/s) | 1.79 (± 0.039) | 1.78 (± 0.036) |
| Cadence (steps/min) | 121 (± 1.18) | 122 (± 1.81) |
| Stride length (m) | 0.92 (± 0.024) | 0.83 (± 0.032) |

| | | |
|---|---|---|
| Stance phase (% GC) | 62.1 (± 0.83) | 60.4 (± 1.64) |
| Single support phase (% GC) | 39.3 (± 1.68) | 38.2 (± 0.75) |

**Normal subject**

| | **left** | **right** |
|---|---|---|
| Velocity (m/s) | 1.56 (± 0.033) | 1.58 (± 0.046) |
| Cadence (steps/min) | 119 (± 3.23) | 119 (± 3.29) |
| Stride length (m) | 0.80 (± 0.041) | 0.81 (± 0.030) |
| Stance phase (% GC) | 59.8 (± 1.60) | 60.0 (± 1.16) |
| Single support phase (% GC) | 39.4 (± 1.14) | 40.2 (± 2.94) |

## 6.2 Comparison normal subject and amputees

### 6.2.1 Ground reaction forces

6.2.1.1 Vertical force component

#### *Right side*

From Figure 6.1 it can be seen that the normal subject presents a ground reaction force which shows two peaks during the entire stance phase.

The first one, after heel-strike, presents a value of 12.14 N/kg (at 13% of the gait cycle), whereas the second peak occurs at 45% of the gait cycle (10.35 N/kg).

The amputee group (especially A2) shows the same pattern with a small delay. A2 presents a negative peak that is smaller than normal group (3.97 N/kg at 34% of the gait cycle).

#### *Left side*

In the sound side A2 presents a greater peak after initial contact (16.03 N/kg at 13% of the gait cycle) than normal group (12.26 N/kg at 14% of the gait cycle).

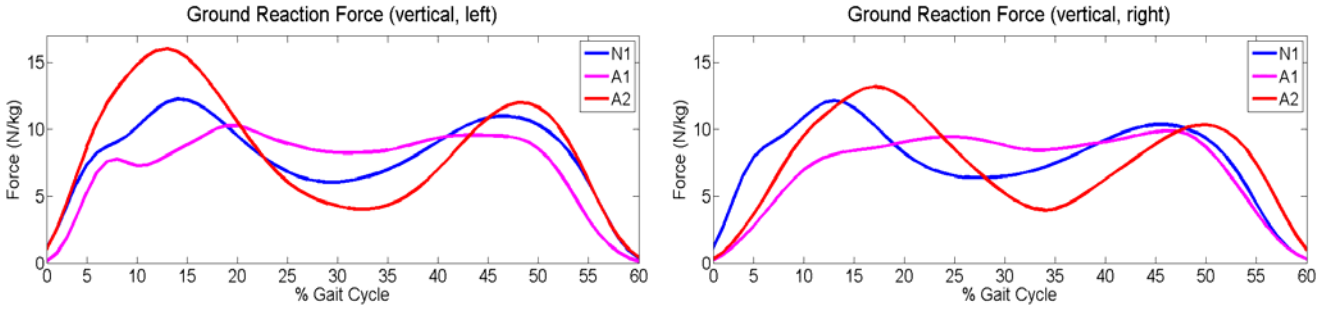


*Figure 6.1. Vertical component of the ground reaction force during stance phase.*

### 6.2.1.2 Anterior-posterior force component

***Right side***

N1 shows a posterior peak of 2.24 N/kg when the heel is in contact with the ground (9% of the gait cycle), whereas the anterior peak occurs at 52% of the gait cycle (2.51 N/kg).

A1 presents peaks that are smaller than N1, while A2 shows a small delay.

***Left side***

In the left side there are not differences between the patterns.

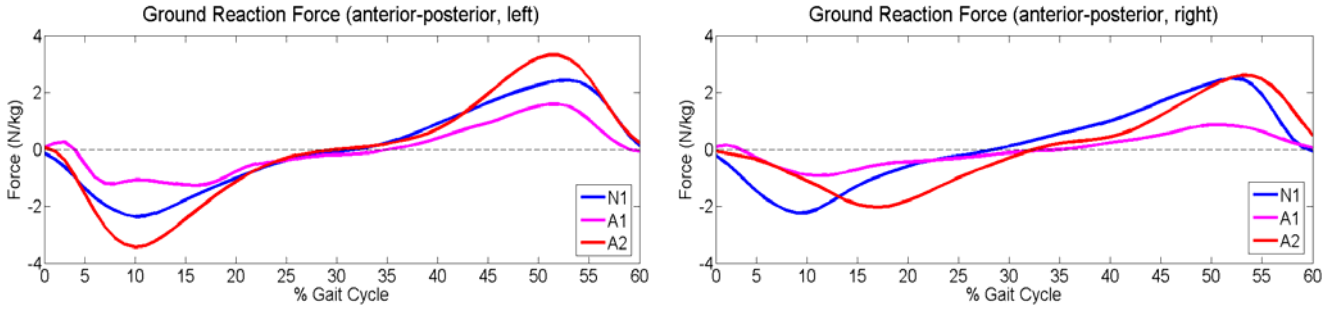


*Figure 6.2. Anterior-posterior component of the ground reaction force during stance phase.*

6.2.1.3 Medial-lateral force component

***Right side***

From Figure 6.3 it can be seen that the N1 shows a lateral thrust after initial contact (0.17 N/kg at 3% of the gait cycle).

After initial loading the normal group does not present a medial peak, but only after the mid-stance (0.64 N/kg at 43% of the gait cycle). Before push-off it can be seen that there are some little lateral forces.

***Left side***

In the left side the patterns of N1 and A2 are very similar.

After initial contact A1 presents a great lateral loading after heel-strike (0.94 N/kg at 6% of the gait cycle).

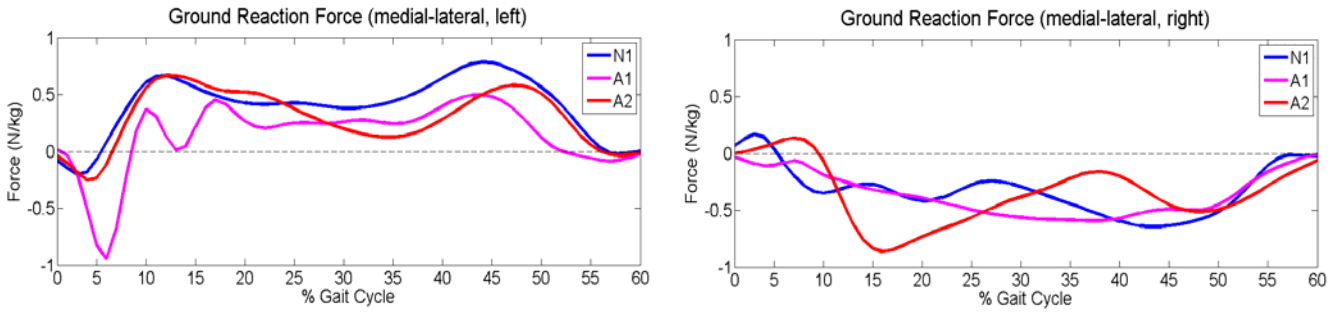


*Figure 6.3. Medial-lateral component of the ground reaction force during stance phase.*

**6.2.2 Joint angles**

6.2.2.1 Knee Flexion

***Right side***

In the normal subject, after initial contact, the knee is flexed. During the weight acceptance there is a flexion of the knee of 17.33° (15% of the gait cycle).

After this phase the knee extends until 3.32° (42% of the gait cycle). At 72% of the gait cycle the knee presents a second flexion (59.5°).

The knee of A2 is already flexed after the initial contact (15.74° at heel strike).

The shape presented by A2 related to the flexion pattern is the same of that one showed by N1.

A1 does not present the first peak of flexion related to the weight acceptance, while the second peak of flexion is greater than N1 (73.04° at 72% of the gait cycle).

### *Left side*

In the normal subject the angles that the left knee shows are the same of the right one.

There is a great extension of the knee (10.27° at 43% of the gait cycle).

The amputee group shows a delay in the two periods when the knee is extending.

The first flexion of the knee is great in A2 (29.58° at 17% of the gait cycle) than in the normal group (19.53° at 15% of the gait cycle).

A greater second knee flexion in the amputee A2 happens also during the swing phase (68.74° at 74 % of the gait cycle for A2, 54.13° at 72% of the gait cycle for N1).

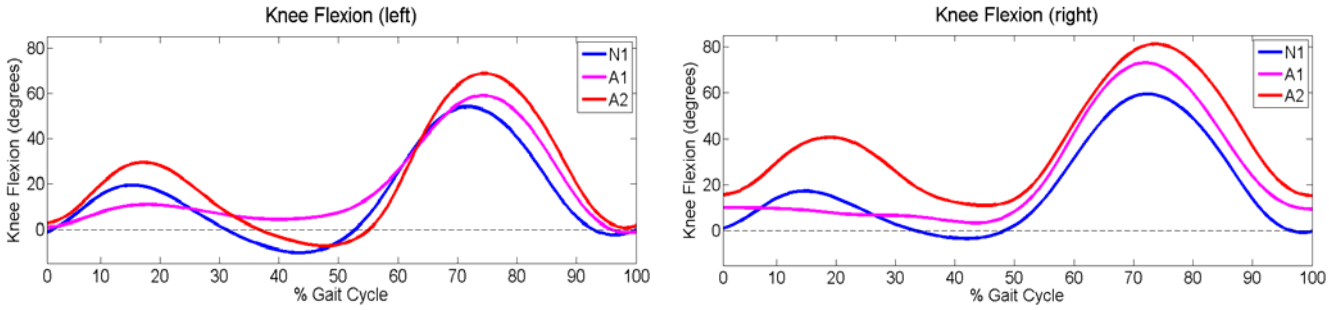


*Figure 6.4. Knee flexion-extension during stance phase.*

6.2.2.2 Hip Flexion

### *Right side*

At heel strike the right hip of the normal subject is already flexed 23.11°, and the following maximal extension is 23.27° (at 51% of the gait cycle). After this phase there is a rapid flexion (23.33° at 100% of the gait cycle).

The flexion of the right hip of the amputee group shows the same shape of the normal group.

A particular difference is that the curve presented by A2 is traversed about 15-20°.

### *Left side*

There are not so many differences from the right and the left flexion of the hip. The patterns and the ranges of the angles are the same.

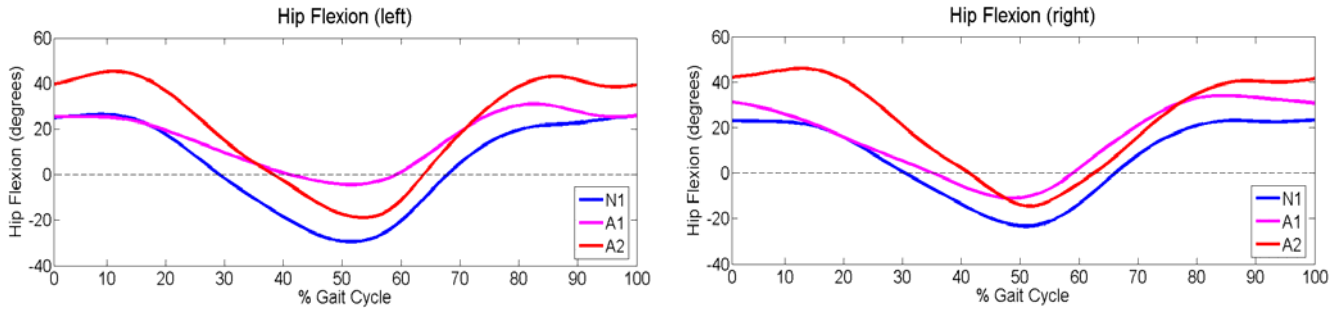


*Figure 6.5. Hip flexion-extension during stance phase.*

6.2.2.3 Hip Abduction

### *Right side*

After initial contact the hip of N1 is already abducted (1.47°). Then there is a small adduction of the hip (0.95° at 19% of the gait cycle).

After this phase the hip moves into abduction, and it reaches the maximum level after toe-off (6.25° at 66% of the gait cycle).

At the end of the gait cycle the abduction of the hip comes back to low values (2.44°).

In the amputee A2, during heel strike the hip is already abducted. After that, the hip starts to move into adduction. The hip continues to be adducted for a while, then it moves into abduction, and it shows the maximum abduction at 69% of the gait cycle (8.95°).

### *Left side*

After initial contact the left hip of N1 is already abducted. There is a small abduction after the heel-strike phase (2.12° at 7% of the gait cycle). Then, adduction of the hip occurs (9.76° at 46% of the gait cycle).

After toe-off the hip is abducted (2.2° at 72% of the gait cycle).

A1 presents a smaller adduction peak than the right limb.

A2 does not present particular differences with the amputee side.

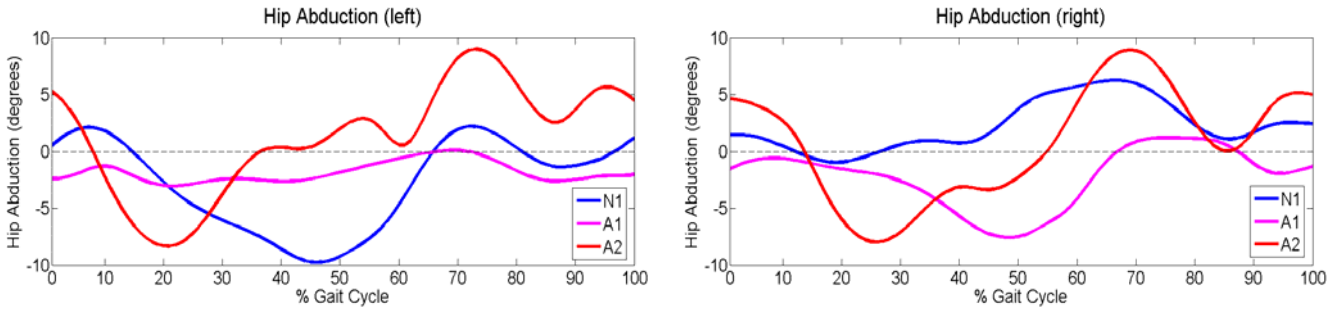


*Figure 6.6. Hip abduction-adduction during stance phase.*

### 6.2.3 Joint moments

6.2.3.1 Knee Flexion Moment

### *Right side*

The normal subject shows an extension moment after heel-strike (0.48Nm/kg at 4% of the gait cycle). After this phase there is a small flexion moment (0.13 Nm/kg at 11% of the gait cycle).

The following extension moment of the knee is greater than usual (0.6 Nm/kg at 39% of the gait cycle).

After the mid-stance the force passes in front of the knee (until toe-off), generating an extension moment.

The amputee subjects present a knee flexion moment that is very close to zero.

### *Left side*

N1 shows the same knee flexion moment of the right side. The shape of the curve is equal. The differences with the contralateral side are a greater flexion moment (0.38 Nm/kg at 15% of the gait cycle), and a greater second extension moment (0.83 Nm/kg at 43% of the gait cycle).

A1 presents a low knee flexion moment, while A2 shows a pattern that is very similar to N1.

The first extension moment of A2, after initial contact, is greater than normal subject (0.75 Nm/kg at 4% of the gait cycle), and the second negative peak (knee flexion moment) before the toe-off is smaller (0.66 Nm/kg at 45% of the gait cycle).

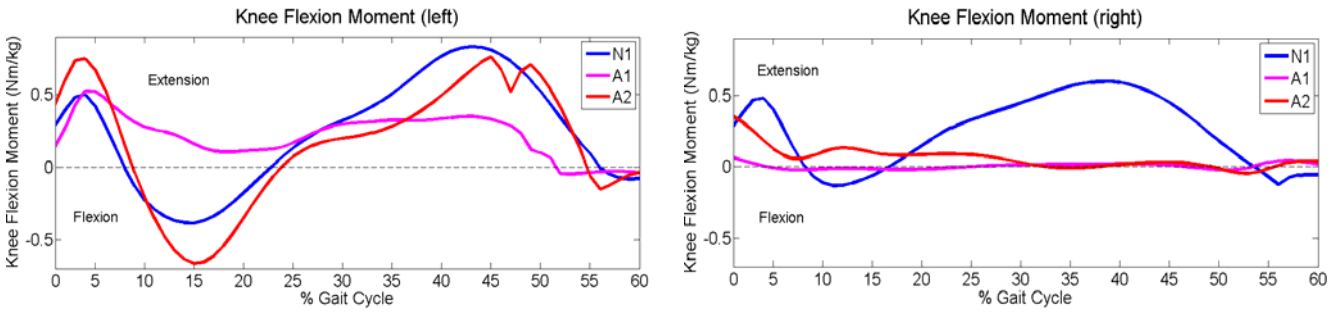


*Figure 6.7. Knee  moment in the sagittal plane, during stance phase.*

6.2.3.2 Hip Flexion Moment

### *Right side*

In the normal subject, after initial contact, the ground reaction force passes quite far anterior to the hip joint. This fact produces a flexion moment (1.24 Nm/kg at 4% of the gait cycle).

During the mid-stance the distance from the ground reaction force and the hip is reduced. After this, the force goes behind the hip creating an extension moment (0.92 Nm/kg at 49% of the gait cycle).

The amputee subjects show a different pattern. The range is smaller than normal group, and after initial contact there is not a flexion moment. The peak of the extension moment that occurs before the toe-off is missing.

### *Left side*

The normal group does not present important differences compared to the right side. Moreover, the range is the same.

The amputee group shows a completely different pattern from the right side, especially A2.

The shape of the curve, that represents the flexion moment of the hip, is very similar to that one of the normal subject.

After initial contact A2 presents a greater flexion moment than N1 (2.04 Nm/kg at 11% of the gait cycle).

During mid-stance and before toe-off the characteristics of the patterns are the same of the normal subject.

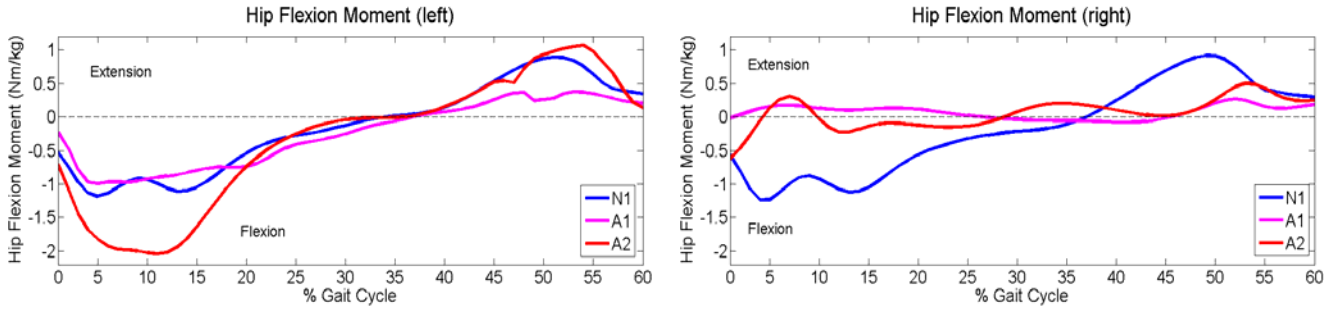


*Figure 6.8. Hip moment in the sagittal plane, during stance phase.*

6.2.3.3 Hip Abduction Moment

### *Right side*

The hip moment in the frontal plane showed by N1 presents two peaks of abduction. The first one occurs at 13% of the gait cycle (0.53 Nm/kg), and the second one at 42% of the gait cycle (0.45 Nm/kg).

From Figure 6.9 it become obvious that negative peaks occurs during the mid-stance (0.19 Nm/kg at 27% of the gait cycle).

The amputee group shows a completely different pattern. The hip abduction moment presents values that are negative or null.

### *Left side*

In the left hip the abduction moment shows the same pattern in the normal subject. There is a greater abduction moment before push-off (0.71 Nm/kg for the normal group at 45% of the gait cycle).

The amputee subjects in the sound side present an abduction moment of the hip that is more similar to N1, if compared with the amputee side.

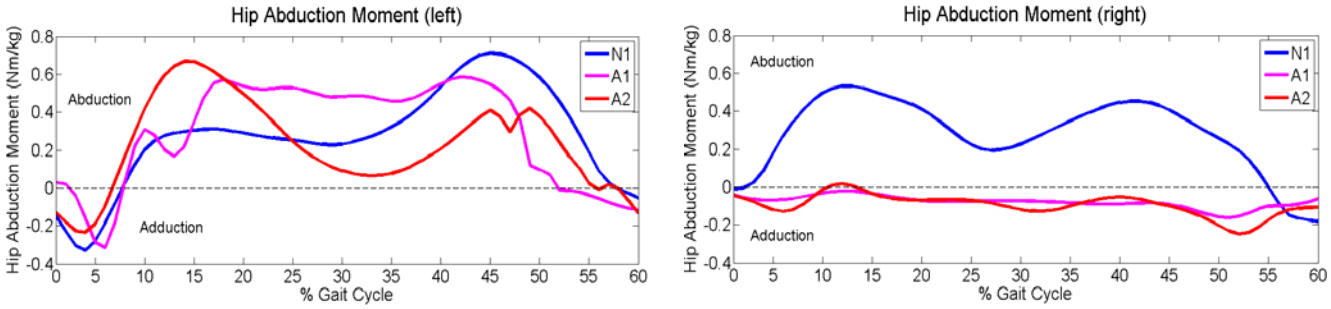


*Figure 6.9. Hip  moment in the frontal plane, during stance phase.*

## 6.2.4 Power

6.2.4.1 Knee Flexion Power

### *Right side*

The knee of the normal subject presents a generation of power after heel-strike (1.12 W/kg at 4% of the gait cycle).

In the following phase the ground reaction force is located behind the knee, and it creates a flexion moment while the knee is flexing. The quadriceps is working eccentrically, and there is a consequent absorption of power that, in this case, shows a small value (0.25 W/kg at 10% of the gait cycle).

At 20% of the gait cycle there should be a generation of power, but N1 does not show it (0 W/kg at 16% of the gait cycle).

Before push-off the ground reaction force is behind the knee, and it creates a flexion moment. In this period of time the knee is flexing. This fact generates an absorption of power (0.72 W/kg at 56% of the gait cycle).

The amputee subjects show a completely different pattern. The values related to generation and absorption of power are almost null, confirming the results of the previous studies of Winter et al. (1988), and Powers et al. (1998).

### *Left side*

On the left side N1 shows the same pattern of the right one. In the case of the amputee group, A1 presents values that are low, while A2 has a pattern that is similar to N1.

The first positive peak of A2, that means a generation of power, is greater than N1 (2.99 W/kg at 5% of the gait cycle, while 1.68 W/kg at 4% of the gait cycle in the normal subject).

Also the second generation peak of power is greater in A2 than in N1 (1.01 vs. 0.41 W/kg at 19% of the gait cycle).

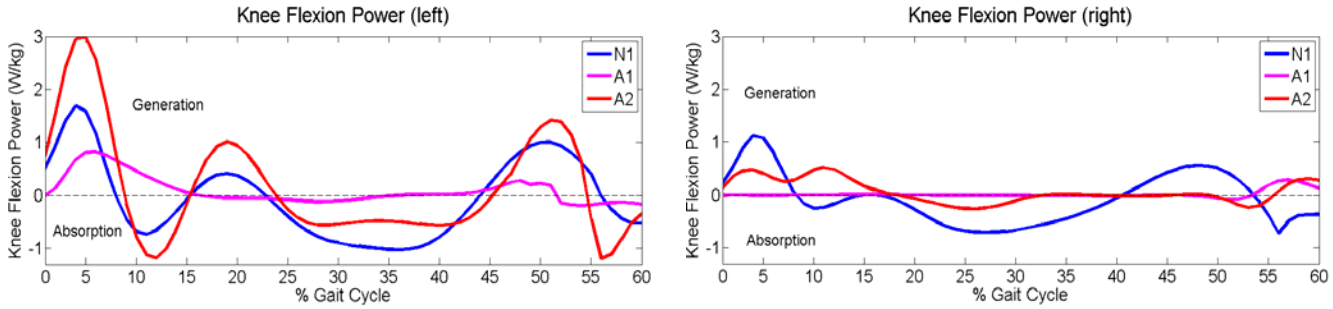


*Figure 6.10. Knee power in the sagittal plane.*

6.2.4.2 Hip Flexion Power

### *Right side*

After initial contact the hip shows a short period of time with flexion velocity coupled with a flexion moment. This is the cause of the initial absorption of power after heel-strike. The normal subject presents zero values, but not a negative peak.

After this phase, the hip starts to extend, while the moment is trying to flex the hip. The result is a power generated by the hip extensors (1.44 W/kg at 17% of the gait cycle).

After this positive peak, there is a change from flexion moment to extension moment. The hip is still flexing, and the result is an absorption of power related to an eccentric contraction of the hip flexors.

The amputee group shows some differences. The range of the values is very restricted.

### *Left side*

In the normal subject there are no marked differences from the right side. After heel-strike there is a greater absorption of power than in the right side (0.59 W/kg at 5% of the gait cycle).

The amputee group shows a completely different pattern from the right side.

A1 shows very low values, while A2, after initial contact, presents a great absorption of power (2.71 W/kg at 5% of the gait cycle) followed by a generation of power (3.58 W/kg at 16% of the gait cycle).

Before push-off A2 shows a peak of generation of power (2.71 W/kg at 56% of the gait cycle) that N1 does not present.

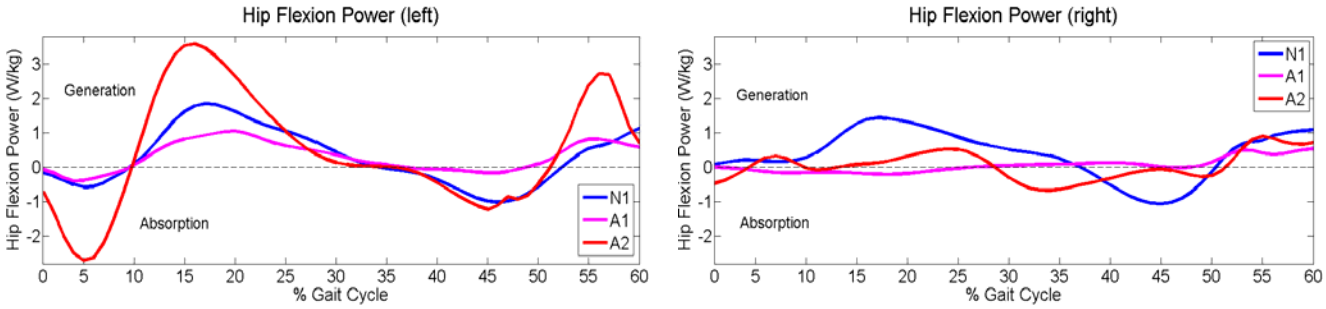


*Figure 6.11. Hip power in the sagittal plane.*

6.2.4.3 Hip Abduction Power

### *Right side*

The normal subject presents an absorption of power after initial contact (0.17 W/kg at 12% of the gait cycle). Before the push-off there is a positive peak that demonstrates a generation of power of 0.33 W/kg (at 46% of the gait cycle).

The amputee group shows, as in the case of knee and hip flexion, a different pattern from the normal subject. Also in this instance the values are low, and the peaks of power absorption and generation are missing.

### *Left side*

The pattern of N1 presents negative values until the phase before push-off, where there is a peak of power generation (0.51 W/kg at 50% of the gait cycle).

From Figure 6.12 it can be seen that A2 presents a generation of power after heel-strike (0.37 W/kg at 4% of the gait cycle), and a following negative peak that demonstrates an absorption of power (0.79 W/kg at 12% of the gait cycle).

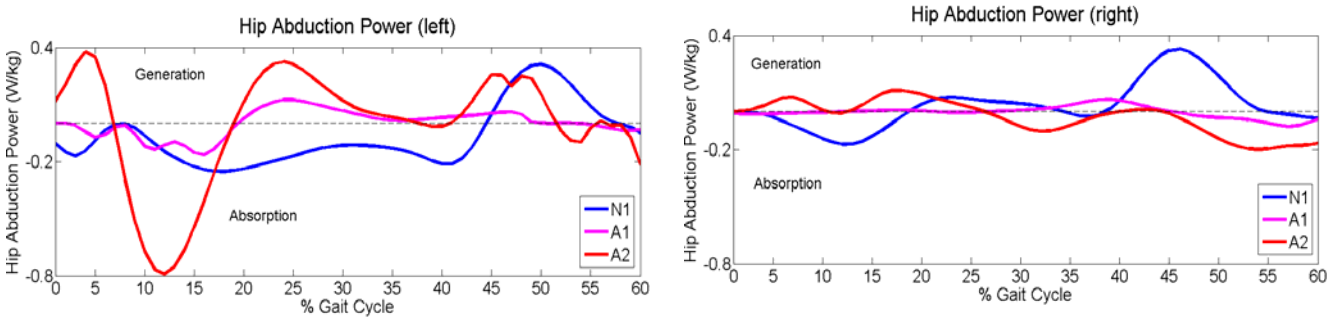


*Figure 6.12. Hip power in the frontal plane.*

### 6.2.5 Muscular Activity

6.2.5.1 Anterior thigh muscles

**Vastus Lateralis**

***Right side***

From Figure 6.13 it becomes obvious that the vastus lateralis in the normal subject is active in the first half of the stance phase.

After initial contact N1 shows a contraction of the vastus lateralis that generates a force of 13.06 N (at 13% of the gait cycle) in the inferior section, and 299.6 N (at 13% of the gait cycle) in the superior section.

It can be seen that the vastus lateralis of the amputee subjects is not active during the stance phase.

***Left side***

The normal subject generates a force of 21.59 N at 14% of the gait cycle in the inferior section, while the superior part of the muscle produced a contraction of 499.3 N at 14% of the gait cycle.

A2 in this case shows an activation of the vastus lateralis that is greater than N1 (37.08 N at 14% of the gait cycle for the inferior section, and 861.8 N at the 14% of the gait cycle for the superior section).

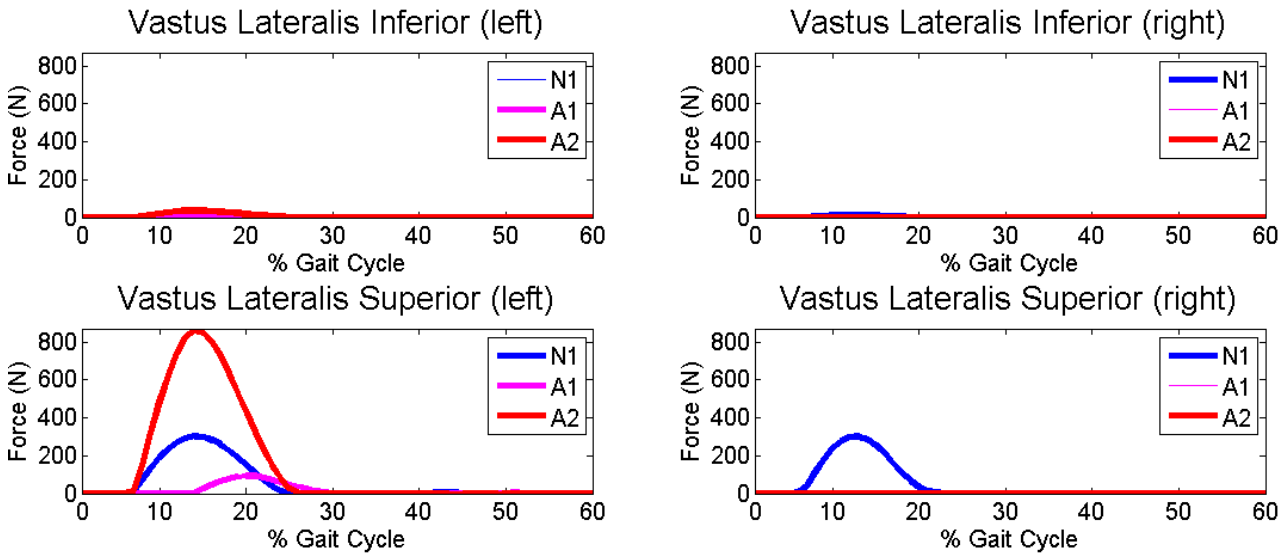


*Figure 6.13. Vastus lateralis activation during stance phase.*

**Vastus Medialis**

### *Right side*

The same results are related to the vastus medialis. From Figure 6.14 it becomes obvious that the normal subject presents a contraction of this muscle during the first half of the stance phase. The inferior part of the muscle generates a force of 19.38 N, 73.24 N the middle part and 53.43 N the superior (at 13% of the gait cycle).

The amputee group does not present activation of this muscle during this period of time.

### *Left side*

The left vastus medialis of the amputee A2 is more active than normal group (54.54 N in the inferior section, 208.1 N in the middle, 152.9 N in the superior at 14% of the gait cycle).

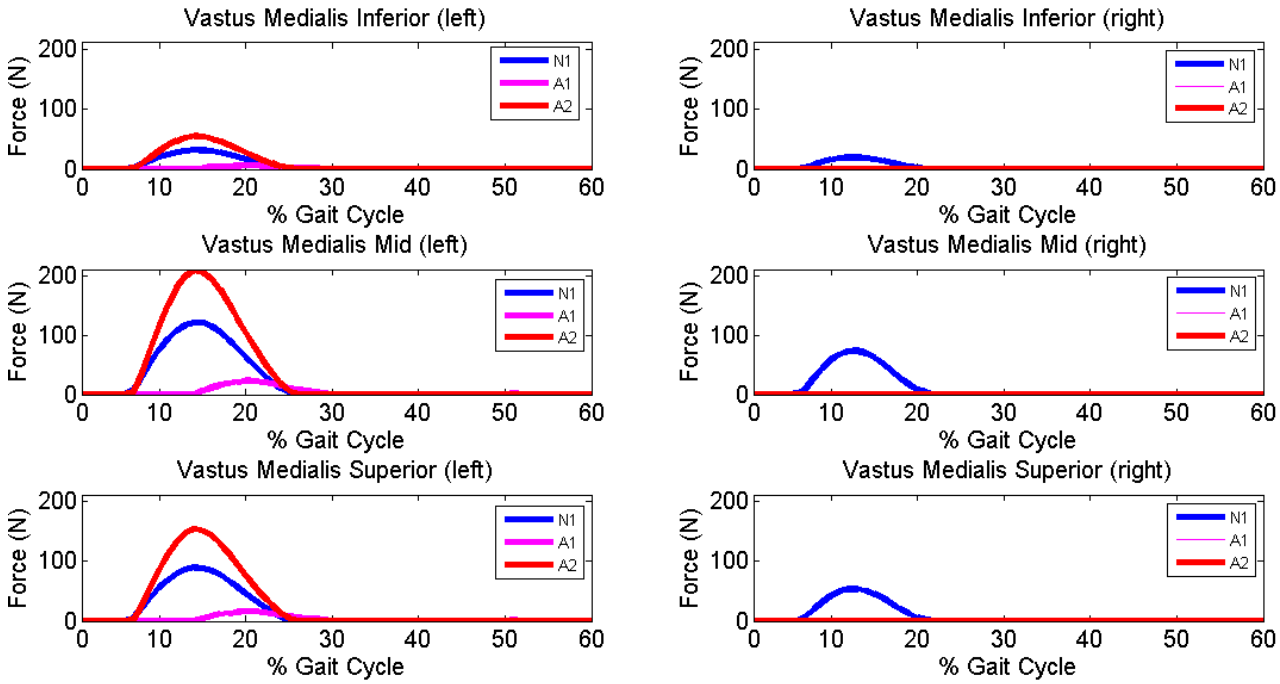


*Figure 6.14. Vastus medialis activation during stance phase.*

6.2.5.2 Posterior thigh muscles

**Biceps Femoris Caput Longum**

### *Right side*

From Figure 6.15 it can be seen that biceps femoris caput longum presents a great activity during the first part of the stance phase.
The normal subject shows the maximal activation at 4% of the gait cycle (517.3 N), but the muscle is still active until mid-stance.
The amputee group presents a smaller activation of the biceps femoris caput longum, and after initial contact the activity of this muscle decreases to lower values.

### *Left side*

In the left side the N1 shows the same pattern of the right side.
A1 presents an activity that is comparable to N1, and A2 shows a great contraction of the biceps femoris caput longum (768.7 N at 4% of the gait cycle).

**Biceps Femoris Caput Breve**

### *Right side*

In the normal group the biceps femoris caput breve is active during almost all the stance phase. From Figure 6.15 it becomes obvious that is not a great activation (the maximum value is 84.17 N after heel-strike).
Also the amputee subjects present a small, but constant, activation of this muscle.

### *Left side*

The amputee group shows a greater muscular activation than normal subject, especially after initial contact.

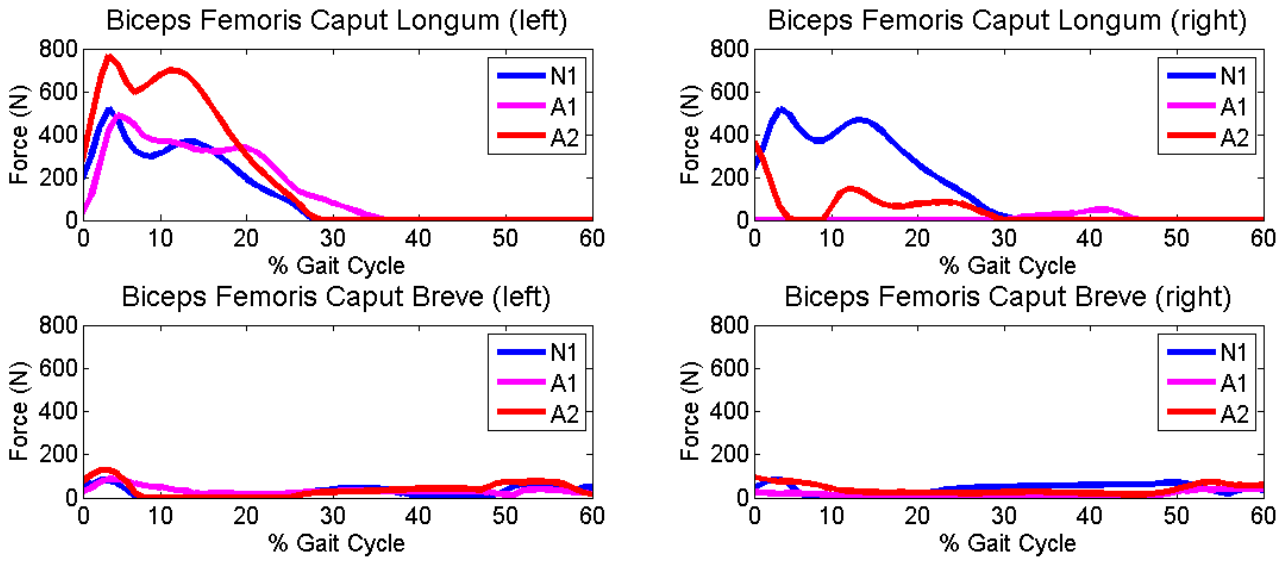


*Figure 6.15. Biceps femoris activation during stance phase.*

### 6.2.5.3 Gluteal region muscles

**Gluteus Maximus Superior**

#### *Right side*

The normal subject presents a great activity after heel-strike (479.3 N at 13% of the gait cycle), whereas the amputee group shows a small activation.

#### *Left side*

It can be seen from Figure 6.16 that in the sound side the amputee group presents a greater activity than N1 (327.4 N at 18% of the gait cycle for A1 and 724.7 N at 12% of the gait cycle for A2).

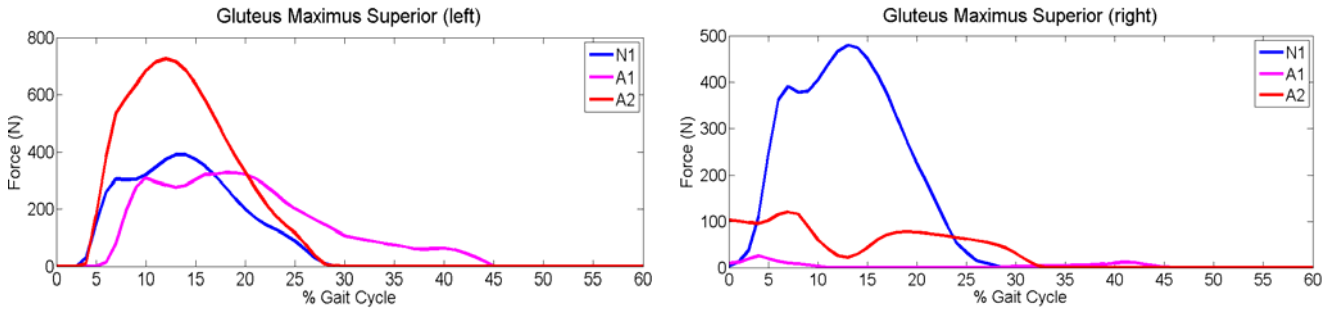


*Figure 6.16. Right gluteus maximus (superior) activation during stance phase.*

## 6.3 Comparison amputee group and virtual amputee

### 6.3.1 Joint moments

6.3.1.1 Knee Flexion Moment

***Right side***

The virtual amputee does not show the knee extension moment after initial contact.

The extension moment that occurs at 39% of the gait cycle shows a great value (0.63 Nm/kg), while the flexion moment of the amputee's knee is almost zero.

***Left side***

In the case of the sound limb the patterns presented by the amputee group and the virtual amputee are very similar.

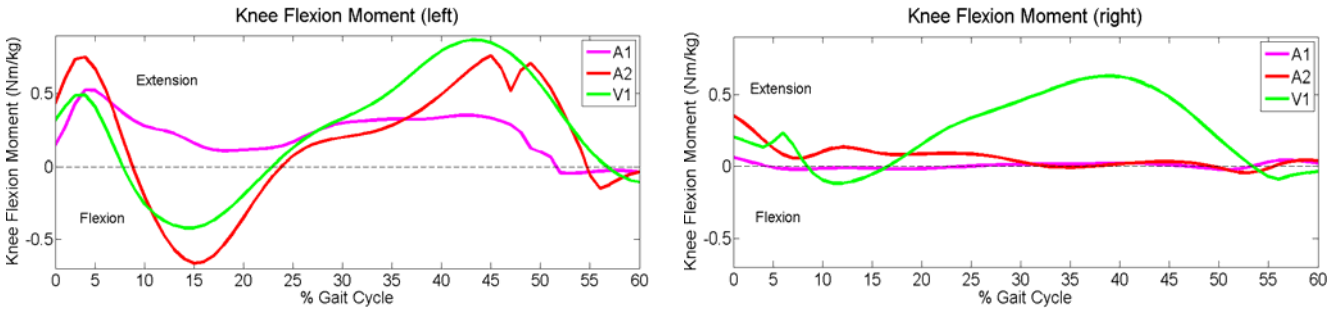


*Figure 6.17. Knee moment in the sagittal plane, during stance phase.*

6.3.1.2 Hip Flexion Moment

***Right side***

The virtual amputee presents a flexion moment after initial contact (1.16 Nm/kg at 13% of the gait cycle), whereas the amputee group shows a reduced moment during all the stance phase.

### *Left side*

The patterns are very similar. The amputee A2 presents a greater flexion hip moment after heel-strike than the virtual amputee (2.04 Nm/kg at 11% of the gait cycle vs. 1.21 Nm/kg at 5% of the gait cycle).

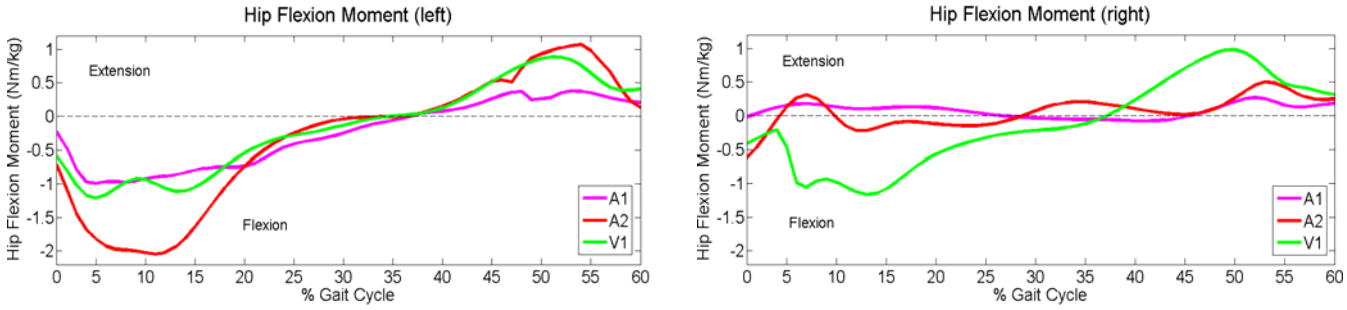


*Figure 6.18. Hip moment in the sagittal plane, during stance phase.*

6.3.1.3 Hip Abduction Moment

### *Right side*

The virtual amputee reports two abduction moment peaks. The first one occurs at 13% of the gait cycle (0.59 Nm/kg) and the second one at 42% of the gait cycle (0.51 Nm/kg).
The amputee group presents a reduced hip abduction moment.

### *Left side*

There are not substantial differences between the amputee group and the virtual amputee in the sound limb. The patterns present almost the same shape.

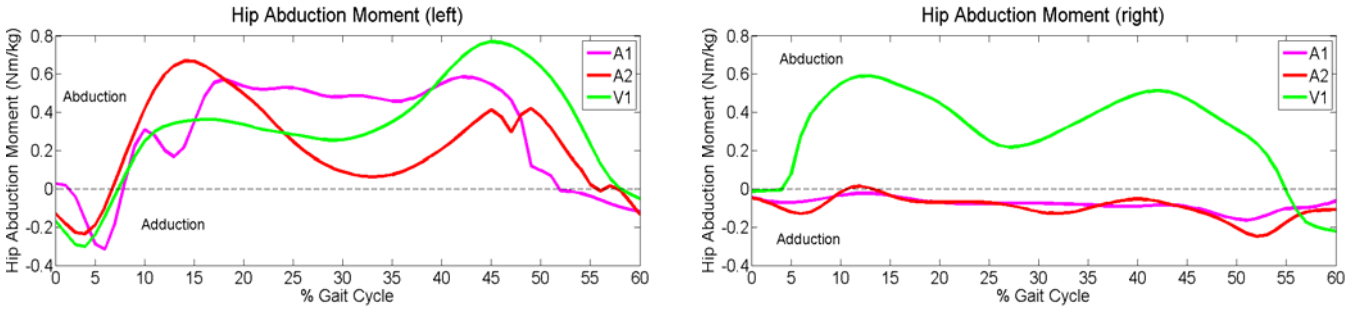


*Figure 6.19. Hip  moment in the frontal plane.*

### 6.3.2 Power

6.3.2.1 Knee Flexion Power

#### *Right side*

The most important differences between the two patterns are related to the absorption and generation peaks that occur respectively at 27% (0.72 W/kg) and 48% (0.60 W/kg) of the gait cycle.

#### *Left side*

The patterns that are shown in the sound limb are similar, especially A2 and V1.

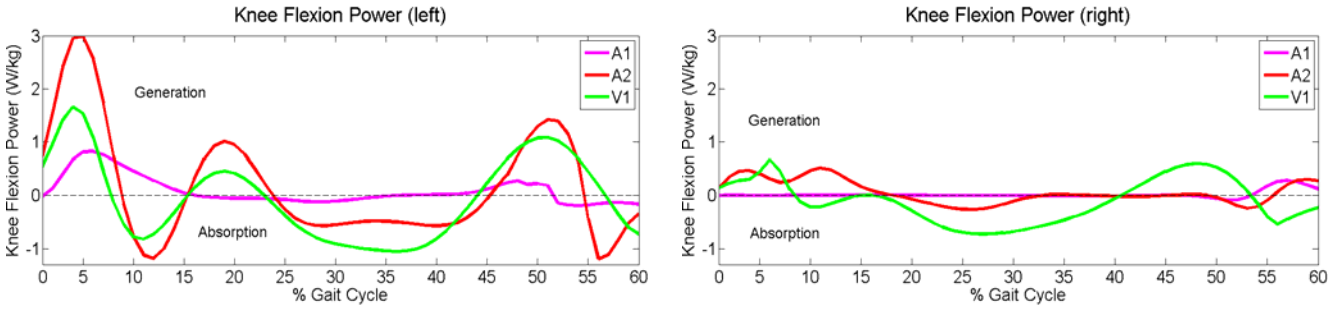


*Figure 6.20. Knee power in the sagittal plane.*

6.3.2.2 Hip Flexion Power

***Right side***

The amputee virtual amputee presents a great generation of power in the first part of the stance phase (1.47 W/kg at 17% of the gait cycle).

***Left side***

The amputee A2 shows a greater absorption of power after initial contact (2.71 W/kg at 5% of the gait cycle) than the virtual amputee (0.59 W/kg at 5% of the gait cycle). From mid-stance until push-off the patterns present the same shape.

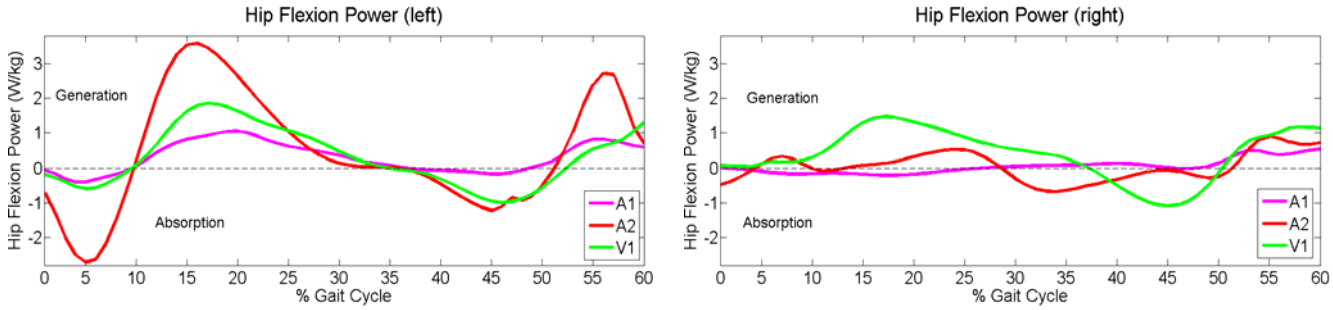


*Figure 6.21. Hip power in the sagittal plane.*

6.3.2.3 Hip Abduction Power

***Right side***

The main difference in the hip abduction power is at 46% of the gait cycle, when a power generation peak occurs (0.38 W/kg).

### *Left side*

The amputee A1 does not present generation of power after heel-strike.

A2 shows a negative peak that demonstrate an absorption of power (0.79 W/kg at 12% of the gait cycle).

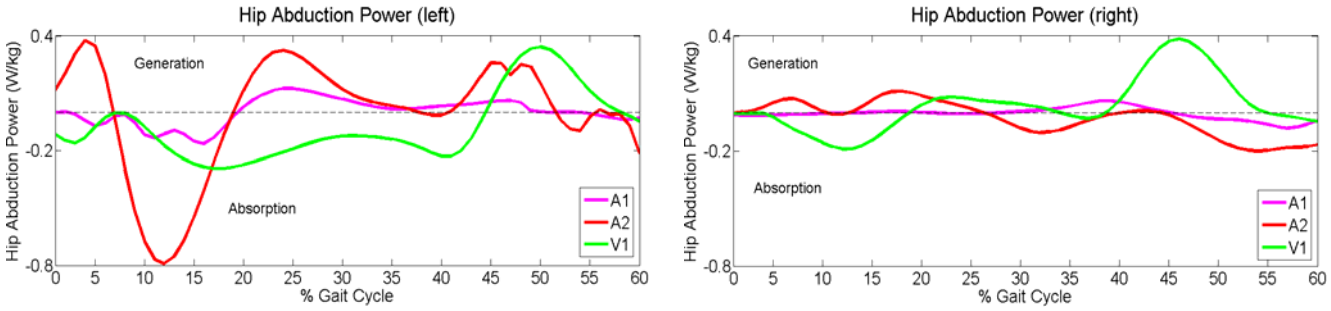


*Figure 6.22. Hip power in the frontal plane.*

### 6.3.3 Muscular Activity

6.3.3.1 Anterior thigh muscles

**Vastus Lateralis**

### *Right side*

The virtual amputee presents a great contraction of this muscle (15.77 N at 12% of the gait cycle for the inferior part, and 358.9 N at 12% of the gait cycle for the superior part), whereas the amputee group does not activate this muscle during the stance phase.

### *Left side*

The virtual amputee shows a greater range of activation than the right side (in both sections, superior and inferior).

The amputee group presents activity in this side.

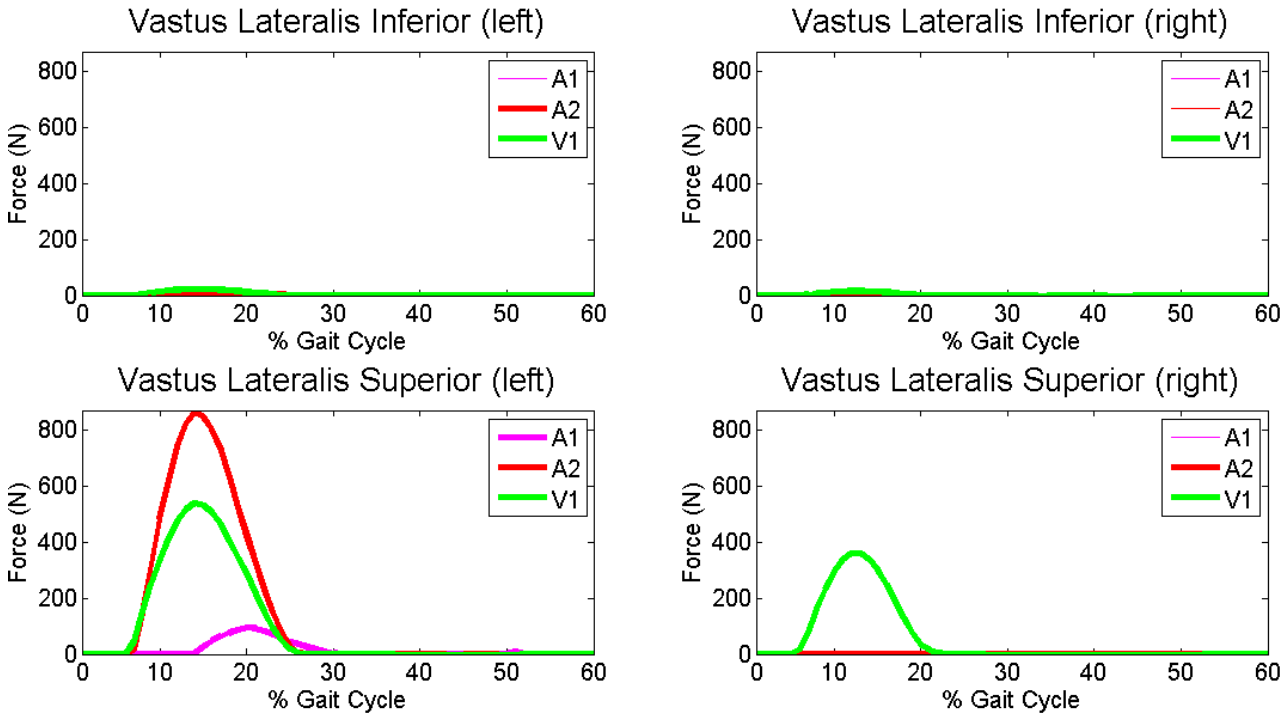


*Figure 6.23. Vastus lateralis activation during stance phase.*

**Vastus Medialis**

## *Right side*

In the case of vastus medialis, similar results to the vastus lateralis have been achieved.

In the right side the amputee group does not present activation of this muscle, while the virtual amputee shows a great activity in the first part of the stance phase (23.52 N for the inferior section, 88.37 N for the middle, 64.17 N for the superior at 12% of the gait cycle).

### *Left side*

In this case the amputee group presents a good activity of the vastus medialis, and from Figure 6.24 it can be seen that the range of activation of A2 and V1 are similar.

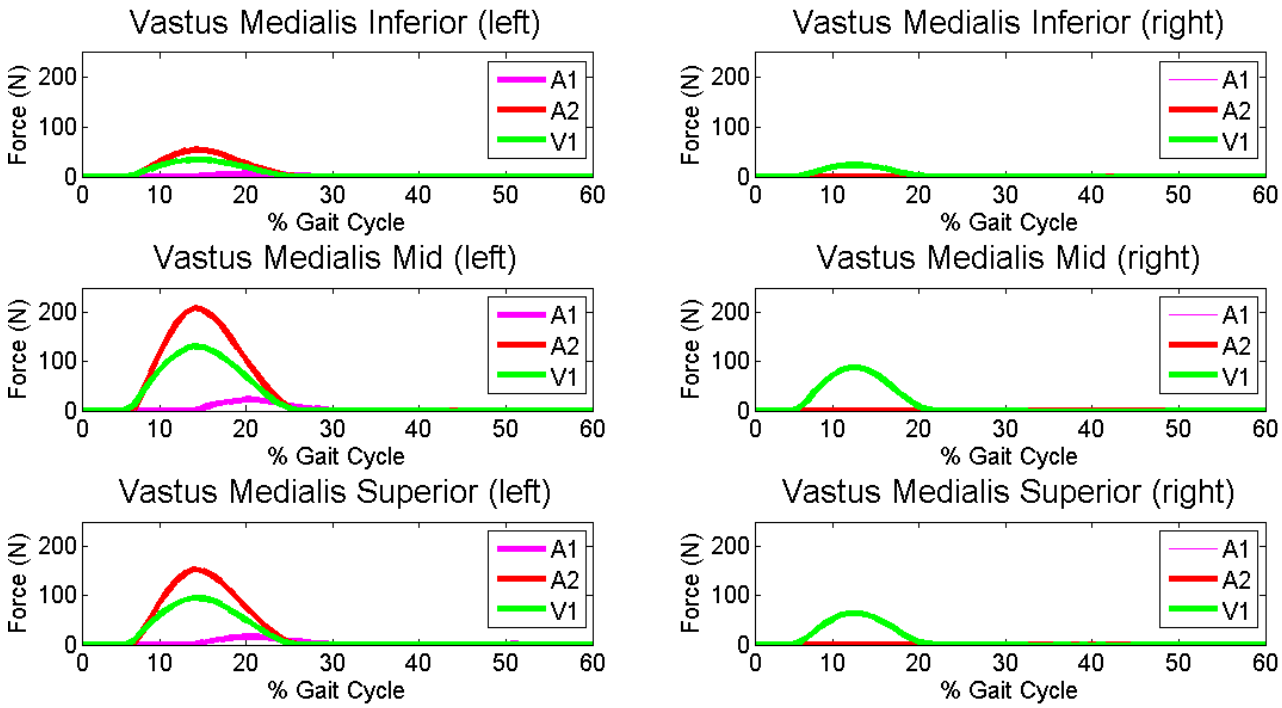


*Figure 6.24. Vastus medialis activation during stance phase.*

6.3.3.2 Posterior thigh muscles

**Biceps Femoris Caput Longum**

### *Right side*

The virtual amputee presents a great activation of the biceps femoris caput longum (667 N at 13% of the gait cycle), whereas the amputees A1 and A2 do not contract this muscle during the first part of the stance phase.

### *Left side*

In the left side the contraction of the biceps femoris caput longum is greater in A2 than in V1 (respectively 768.4 N at 4% of the gait cycle and 542.7 N at 4% of the gait cycle).

**Biceps Femoris Caput Breve**

### *Right side*

The virtual amputee presents a peak of activation in the second part of the stance phase (176.2 N at 46% of the gait cycle).

### *Left side*

The patterns that are shown by the two groups are very similar, and they presents the same shape.

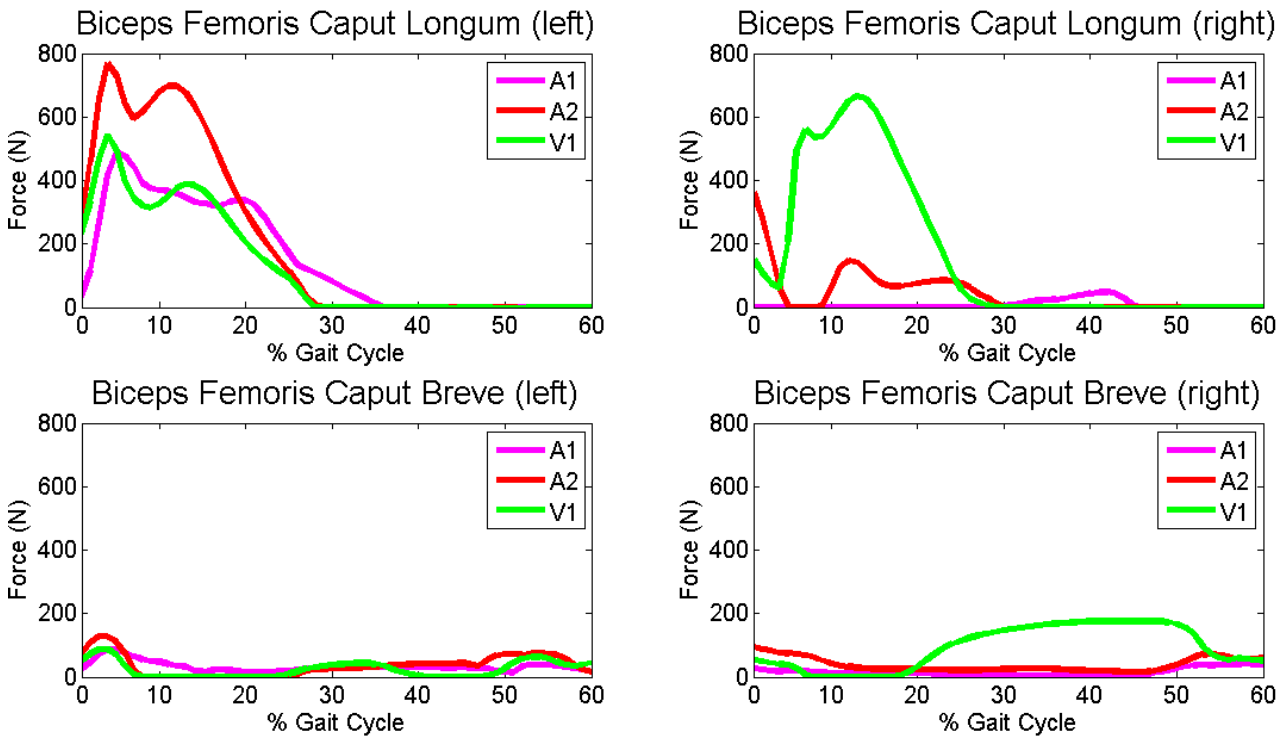


*Figure 6.25. Biceps femoris activation during stance phase.*

6.3.3.3 Gluteal region muscles

**Gluteus Maximus Superior**

### *Right side*

During the first part of the gait cycle the amputee group presents a low activation of the gluteus maximus, while the virtual amputee shows a prolonged peak of activation where the maximum value is 173 N (at 14% of the gait cycle).

### *Left side*

In the left side the period of activation of the gluteus maximus is the same in the two groups. The amputee A2 presents a greater activation (724.7 N at12% of the gait cycle) than the amputee model with healthy kinematics (411.8 N at 14% of the gait cycle).

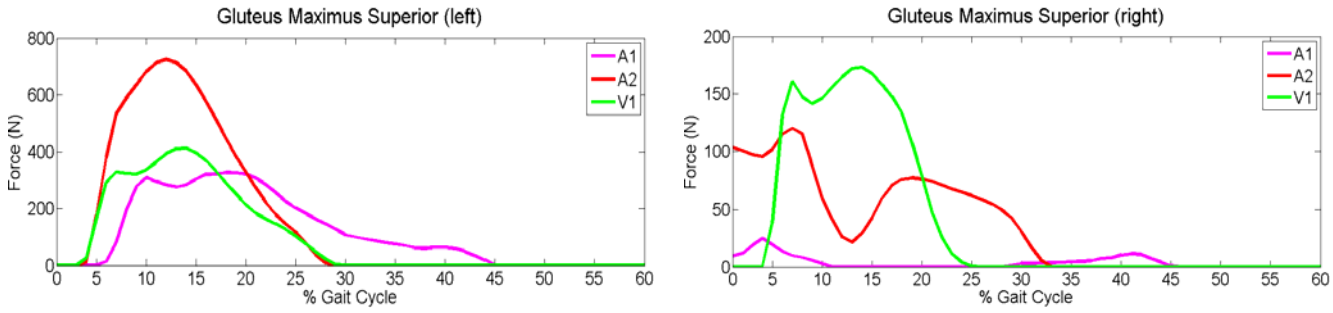


*Figure 6.26. Right gluteus maximus (superior) activation during stance phase.*

## 6.4 Discussion

### 6.4.1 Review of the results

The results of this study show that the trans-tibial amputees do not present important differences in the ground reaction forces.

The main alteration of the results can be evaluated (especially in the amputation side) in the joint angles, reduced moment and power of the knee and hip during the stance phase.

From Figure 6.4 it can be seen that the amputee knee presents a different angle of flexion from the normal group, during the gait cycle.

From Figures 6.7-8-9 it become obvious that in the right side (where there is the amputation) the amputee group presents reduced joint moments, while in the left side the patterns show the same shape.

The same evaluation can be done about the graphs related to the joints power.

The range shown by the amputee group (in the right side) is reduced, and there are not the peaks of power generation and absorption that can be seen in the normal group.

In the left side the results are completely different. The patterns presented by the amputees are similar to the normal. For instance, from Figure 6.12 it can be seen that the shape presented by the amputee group is comparable to the normal group, and the peaks of generation and absorption power are greater.

The same difference from left and right side can be observed in the muscular activity.

The vastus lateralis superior of the amputee group does not present activation in the right side, while in the left limb the activation is greater than normal group (Figure 6.13). The same results can be evaluated in the biceps femoris caput longum and the gluteus maximus superior (Figures 6.15-16).

The same differences in the joint angles, moments of force and power can be observed in the graphs that compare the virtual amputee with the amputee group.

Also the muscular activity presents a substantial difference between the left and right side. In the right side the virtual amputee presents a greater muscular activation than the amputee group, and in the left limb the amputees show a good contraction of the muscles, especially the extensors of the hip.

### 6.4.2 Discussion of the results

It can be seen from Figures 6.1 and 6.2 that the knee and hip flexion of the amputee group (in the amputee side) is traversed up than the normal group.

The differences between normal and amputee group in the hip abduction patterns are the demonstration of the asymmetric gait in the amputees. The variation of the abduction/adduction angle can be a consequence of the movement of the pelvis.

From Table 1 it can be seen that amputee1 shows a short stride length. This particular fact can affect the ground reaction forces and the force moments in the amputee side.

About the ground reaction forces there are not substantial differences between the normal and amputee groups, while the most important differences are related to the force moments and joint powers.

By observing Figure 6.7 it become obvious that at heel-strike the ground reaction force passes anterior to the knee joint, generating an extension moment.

It can be seen that the resulting moment for the amputee group is different, and there is not the first peak of extension. The principal reasons are the first contact of the prosthesis with the force plate, and the following weight acceptance.

In the graphs that represent the knee flexion moment it can be evaluated that the right knee matches what is seen in the studies of Winter et al. and Powers et al., and the left is almost the same, in timing and pattern. There is only the magnitude that shows little differences, especially the first extension moment peak (as it was described before).

The same evaluation can be done about the hip moment in the sagittal plane. The moment on the amputee side is very small and, on the left side (as in the knee flexion moment), it is very similar to healthy.

From Figure 6.9 it becomes obvious that, about the hip abduction moment, the right side shows great differences, while the left side presents a shape similar to normal. These important differences can be evaluated as a “minimization tactic” adopted by the amputees. If the moment is close to zero the gait kinematics are changed in a way that there is no external GRF moment generated at the joint; actually each joint. Thus the evaluation is that the amputees are using the side with amputation passively.

At heel-strike the ground reaction force passes in front of the knee producing an extension moment while the knee is flexing. The result is a generation of power.

This power generation allows the flexion of the knee, rather than hyper-extension, after heel-strike. These evaluation can be confirmed by observing the graphs related to the joints power.

From Figure 6.10 it can be seen that the knee joint is not used to absorb or generate any energy. The amputees are only hobbling or rather pivoting over their amputee leg, and also the power generated and absorbed in the sagittal plane by the hip can confirm this remark.

The graph related to the power generated and absorbed by the hip in the frontal plane shows that energy is much reduced in amplitude, possibly indicating a stiff leg (in the amputee side). The

obvious consequence is that the net “input-output” by this joint with regard to propulsion seems to be reduced. Whereas, in the sound limb, the graph shows that the power absorption is reduced with a power generation for almost the whole stance phase (Figure 6.12).

These results indicate that the role of the opposite hip is shifted from absorption to more generation.

Also the graphs related to the muscular activity present particular differences between normal and amputee groups.

From Figure 6.13 it becomes obvious that the right vastus lateralis is not used during amputee gait. This result supports the interpretation of a passive use of the amputated leg.

Whereas the vastus lateralis of the contralateral limb presents a greater activation than the normal group.

The same evaluation can be observed in the case of the vastus medialis.

From Figure 6.15 it can be seen that the right biceps femoris (caput breve) largely increases force in late stance, indicating higher demands on this muscle, whereas the shape on the healthy side is not change substantially.

The activation of the glutes maximus can explain the differences related to the moment and power that the hip presents in the frontal plane.

The greater activation of the amputee’s gluteus maximus supports the higher demand on the hip muscles on the healthy side.

Important evaluations can be observed from the graphs where the gait of the amputee group and the virtual amputee are compared.

About the moments of force and joints power, there are the same differences that were described before, between the normal subject and the amputee group.

From Figure 6.22, when the healthy kinematics is applied it seems a noticeable higher net power is needed likely to point at an increased activity of hip abductors right.

The main remarks are related to the muscular activity.

It can be seen from the graphs of the activation of the muscles that if an amputee tries to walk like a sound person needs to practice a greater muscular activity.

This is demonstrated by the Figure 6.23 that represents the activation of the vastus lateralis. From this graph it becomes obvious that if the patients would try to walk normally a higher activity is required.

From Figure 6.25 it can be seen that the virtual amputee needs the highest activity in the biceps femoris, which is a hip extensor, while when walking as they usually do the activity is far reduced. That means that aiming at normal/symmetric walking would largely increase the muscular activity and would be energetically disadvantageous.

## 6.5 Conclusions

The development of this model, useful for trans-tibial amputees, confirms part of the theories already demonstrated during previous studies.

The group composed by trans-tibial amputees presents an asymmetric gait.

Moreover, the amputee group demonstrates reduced joint moments and power in the amputee limb.

The asymmetric gait presented by the amputees is due to the greater activity in the sound side.

The advantage that this “amputee model” gives to the operator is that it can be used with healthy kinematics.

With this procedure the user can check the adequacy of the hypothetic symmetric gait of the amputee.

The results demonstrate that an amputee, if he wants to walk like a sound person, has to generate a greater muscular activation, especially in the amputee side.

# Appendix A

## AnyScript code useful for the generation of the prosthesis

```
AnyFolder Prosthesis = {

  AnyFolder &ref = .HumanModel.BodyModel.Right.Leg.Seg;

  AnyFolder &refRightShank=.HumanModel.BodyModel.Right.Leg.Seg
                           .Shank.ScalingNode;

  AnyFolder &refRightJnt=.HumanModel.BodyModel.Right.Leg.Jnt;

  AnyFolder &ProsthesisJnt1=.HumanModel.BodyModel.Right.Leg.Seg

.Prosthetic_Shank.prosthetic_shank_attachment;
  AnyFolder &ProsthesisJnt2=.HumanModel.BodyModel.Right.Leg.Seg
                            .Shank.ScalingNode.shank_attachment;
  AnyFolder &ProsthesisJnt3=.HumanModel.BodyModel.Right.Leg.Seg
                            .Prosthetic_Foot.prosthetic_foot_attachment;
  AnyFolder &ProsthesisJnt4=.HumanModel.BodyModel.Right.Leg.Seg

.Prosthetic_Shank.prosthetic_shankankle_attachment;


  refRightJnt =
  {
     AnyStdJoint Prosthetic_Shank_Jnt =
     {
       AnyRefFrame &ref1 = ..ProsthesisJnt1;
       AnyRefFrame &ref2 = ..ProsthesisJnt2;
     }; // Prosthetic_Shank_Jnt

     AnyRevoluteJoint Prosthetic_Ankle_Jnt =
     {
       //Axis = z;
       //Ref = 0;
       AnyRefFrame &ref3 = ..ProsthesisJnt3;
       AnyRefFrame &ref4 = ..ProsthesisJnt4;
     }; // Prosthetic_Ankle_Jnt

     AnyReacForce AnkleForce =
     {
       Type = On;
       AnyRevoluteJoint &ankle = .Prosthetic_Ankle_Jnt;
     };
  }; // refRightJnt

  refRightShank =
  {
    AnyRefNode shank_attachment =
    {
```

```
      sRel = ({0.02, 0.22, 0.0});
      //ARel = {{1, 0, 0}, {0, 1, 0}, {0, 0, 1}};
    }; // prosthesisAttachment
  }; //refRightShank

  ref =
  {
    AnySeg Prosthetic_Shank =
    {
      //r0 = {0.365, -1.7, 0.12};
      //rDot0 = {0, 0, 0};
      //Axes0 = RotMat(90*pi/180,z)*RotMat(90*pi/180,x)*RotMat(-
20*pi/180,z);
      //omega0 = {0, 0, 0};
      Mass = 2;
      Jii = {0.005, 0.001, 0.005};
      //Jij = {0, 0, 0};
      sCoM = {0, 0.1, 0};
      JaboutCoMOnOff = On;


      //Scaling node this node is used for the scaling of the segment
      AnyRefNode ScalingNode =
      {
        sRel = {0,0,0};

        AnyDrawNode drw =
        {
          RGB = {0,1,0};
        };
      };

      AnyRefNode prosthetic_shank_attachment =
       {
        sRel = {0, 0.2, 0};

        //ARel = {{1, 0, 0}, {0, 1, 0}, {0, 0, 1}};
      };

      AnyRefNode prosthetic_shankankle_attachment =
       {
        sRel = {0.00, 0.00, 0.0};
        //ARel = {{1, 0, 0}, {0, 1, 0}, {0, 0, 1}};
      };

      AnyFunTransform3DIdentity Scale =
      {
      };

      AnyDrawSeg drwseg =
     { //Visible = On;
        //Opacity = 1;
        //RGB = {0.91796875, 0.76953125, 0.06640625};
        //Transparency = 1;
        /*TextFont = {
        RGB = {0, 0, 0};
        FontName = "Times New Roman";
        Height = 10;
```

```
        Width = 4;
        Bold = Off;
        Italic = Off;
        };*/
        //NodesVisible = On;
        //InertiaScale = 1;
        //AnyStyleDrawMaterial &<Insert name0> = <Insert object
reference
        //(or full object definition)>;
      }; //drwseg
    }; //Prosthetic_Shank

    AnySeg Prosthetic_Foot =
    {
      //r0 = {0.365, -1.7, 0.12};
      //rDot0 = {0, 0, 0};
      //Axes0 = RotMat(90*pi/180,z)*RotMat(90*pi/180,x)*RotMat(-
20*pi/180,z);
      //omega0 = {0, 0, 0};
      Mass = 0.3;
      Jii = {0.0001, 0.0005, 0.0005};
      //Jij = {0, 0, 0};
      sCoM = {0.06, 0, 0};
      JaboutCoMOnOff = On;


      //Scaling node this node is used for the scaling of the segment
      AnyRefNode ScalingNode =
      {
        sRel = {0,0,0};

        AnyDrawNode drw =
        {
          RGB = {0,1,0};
        };
      };

      AnyRefNode prosthetic_foot_attachment =
        {
        sRel = {0.00, 0.00, 0.0};
        // {0.1,0,0};
      };

      AnyFunTransform3DIdentity Scale =
      {
      };

      AnyRefNode HeelContactNodeLow =
        {
        sRel = {0,0,0};
        AnyDrawNode drw = {
          RGB = {0,1,0};
        };
      }; // HeelContactNodeLow

      AnyRefNode ToeLateralContactNode =
        {
        sRel = {0.1,0,0.01};
```

```
        AnyDrawNode drw = {
          RGB = {0,1,0};
        };
      }; // ToeLateralContactNode

//      AnyRefNode TestNode = {
//        sRel = {0.17,0.05,0};
//      };

      AnyDrawSeg drwseg =
      { //Visible = On;
        //Opacity = 1;
        //RGB = {0.91796875, 0.76953125, 0.06640625};
        //Transparency = 1;
        /*TextFont = {
        RGB = {0, 0, 0};
        FontName = "Times New Roman";
        Height = 10;
        Width = 4;
        Bold = Off;
        Italic = Off;
        };*/
        //NodesVisible = On;
        //InertiaScale = 1;
        //AnyStyleDrawMaterial &<Insert name0> = <Insert object
reference
        //(or full object definition)>;
      }; //drwseg
    }; //Prosthetic_Foot
  }; //ref
}; //Prosthesis folder
```

# List of References


Czerniecki, J. M. (1996). Rehabilitation in limb deficiency. 1. Gait and motion analysis. *Arch Phys Med Rehabil,* 77, S3-S8.

Winter, D. A., Sienko, S. E. (1988). Biomechanics of below-knee amputee gait. *J. Biomechanics,* 21(5), 361-367.

Powers, C. M., Rao, S., Perry, J. (1998). Knee kinetics in trans-tibial amputee gait. *Gait and Posture*, 8, 1-7.

Gordon, E. J., Ardizzone, J. (1960). Clinical experiences with the S.A.C.H. foot prosthesis. *Journal of Bone and Joint Surgery*, 42, 226-234.

Edelstein, J. E. (1988). Prosthetic feet: state of the art. *Physical therapy,* 68(12), 1874-1881.

Giakas, G., Baltzopoulos, V. (1997). A comparison of automatic filtering techniques applied to biomechanical walking data. *J. Biomechanics*, 30(8), 847-850.

Damsgaard, M., Rasmussen, J., Christensen, S. T., Surma, E., de Zee, M. (2006). Analysis of musculoskeletal systems in the AnyBody Modeling System. *Simulation Modelling Practice and Theory*, 14, 1100–1111.

Andersen, M. S., Damsgaard, M., MacWilliams, B., Rasmussen, J. (2009). A computationally efficient optimisation-based method for parameter identification of kinematically determinate and over-determinate biomechanical systems. *Computer Methods in Biomechanics and Biomedical Engineering*, 13(2), 171-183.